Structure thermochimique du manteau profond: observations et modèles

Frédéric Deschamps

ETH Zürich

avec …

Jeannot Trampert
Paul Tackley
Joe Resovsky
Takashi Nakagawa

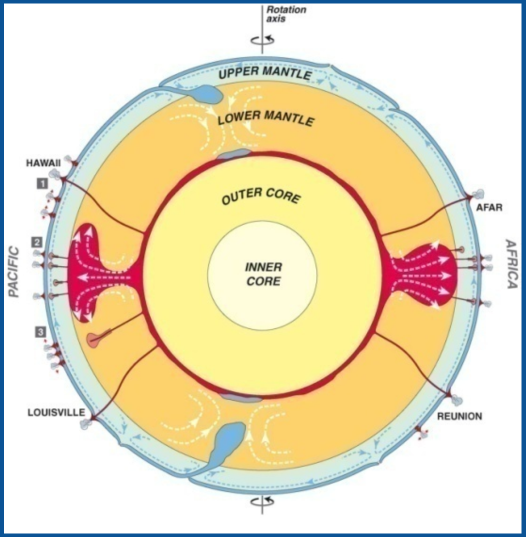

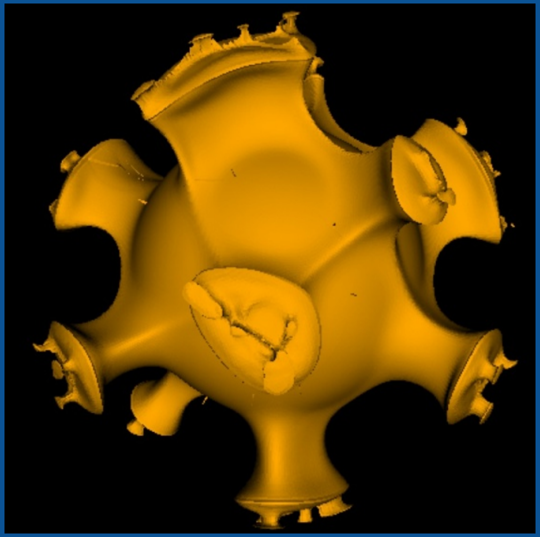

EOST Strasbourg
18 Janvier 2011

"La Terre n'est pas une planète quelconque ! …"

"… On y compte 111 rois (en n'oubliant pas, bien sûr, les rois nègres), **7,000 géographes**, 900,000 businessmen, 7,500,000 ivrognes, 311,000,000 vaniteux, c'est-à-dire environ 2,000,000,000 de grandes personnes"

(Antoine de Saint-Exupéry, Le Petit Prince)

Et c'est une planète dynamique (Tectonique des plaques!)

Linking geophysical observables and geodynamics

Geodynamics is often essential to explain geophysical data sets

Mantle convection and seismic tomography

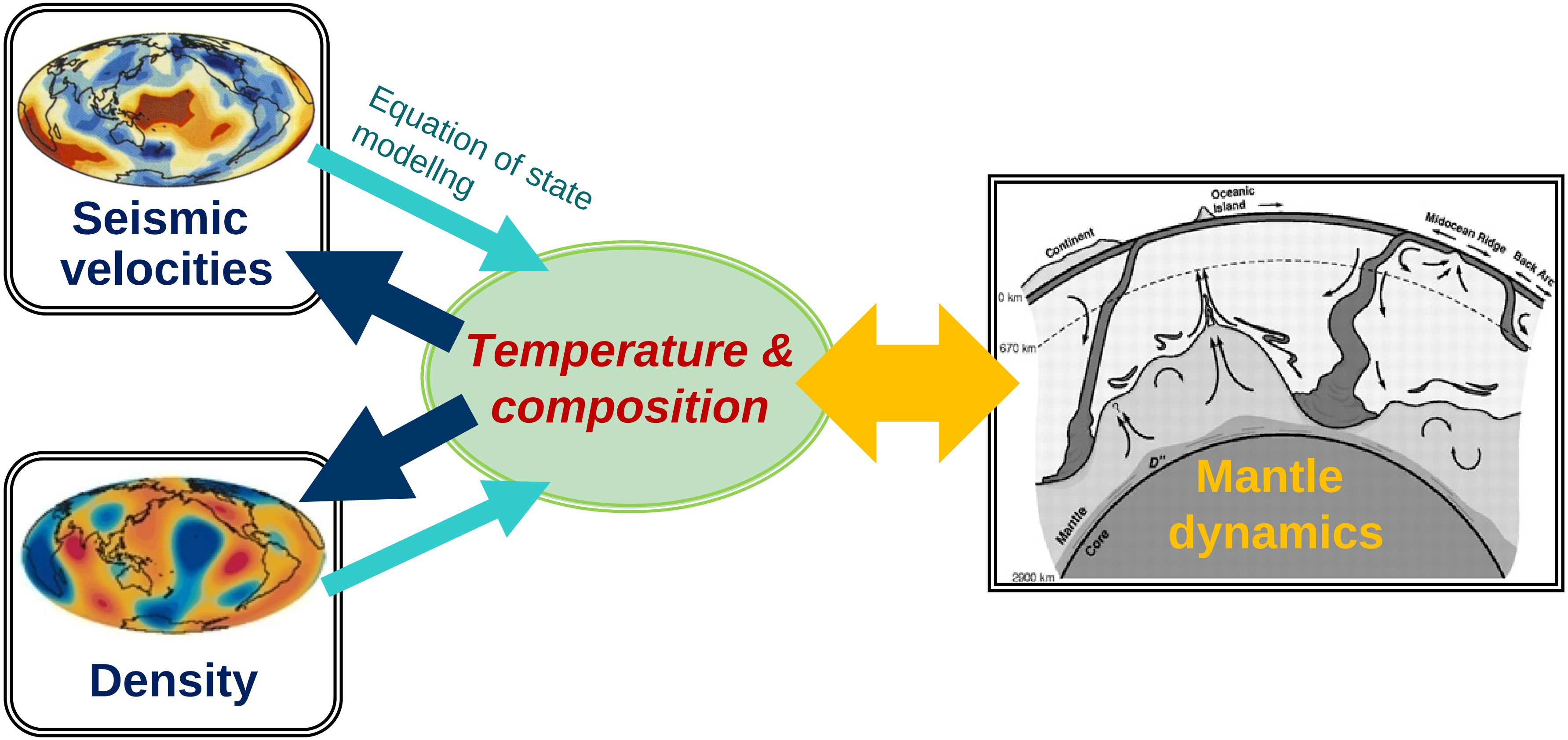

- Mineral physics data and Equation of State modeling.
- Density to break trade-offs between temperature and composition.
- Monte-Carlo search to account for error bars in observations and mineral physics data.

Thermo-chemical structure and dynamics of the Earth's deep mantle

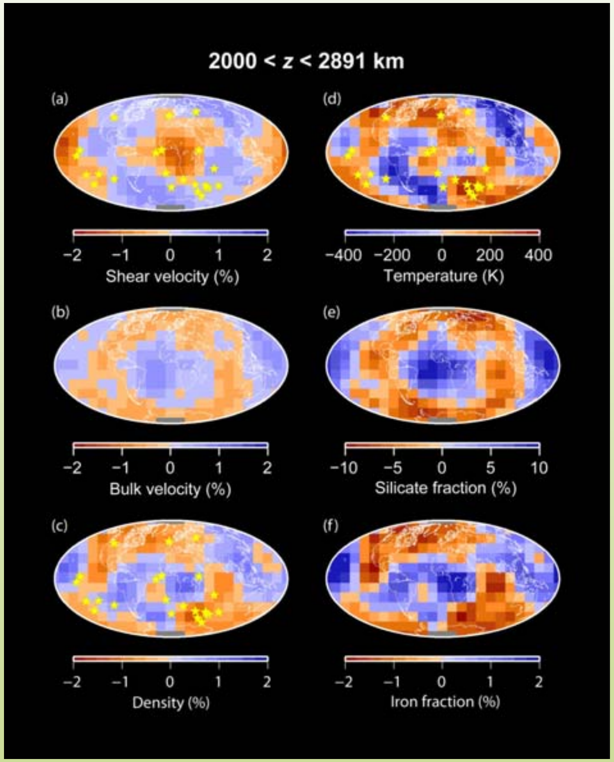

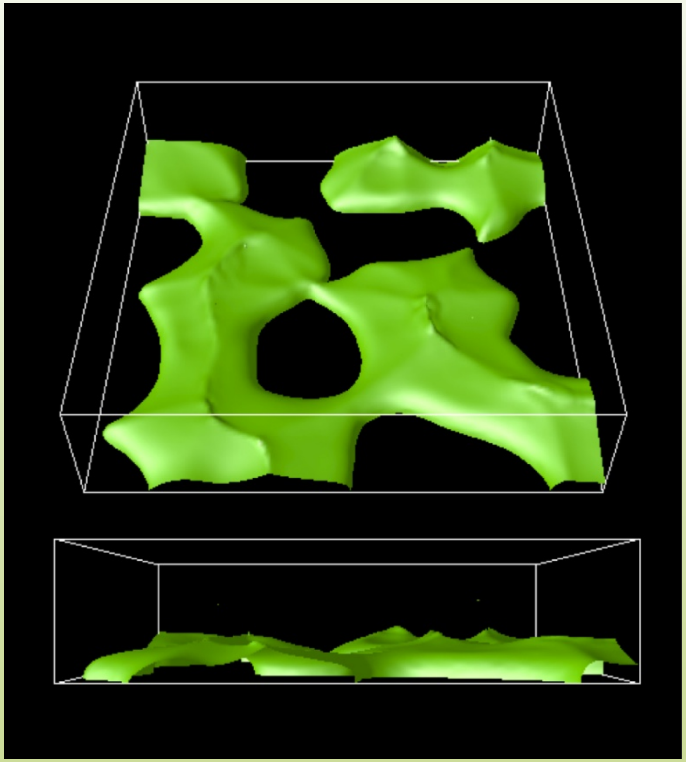

Earth: radial and lateral structure

- Radial structure: well constrained

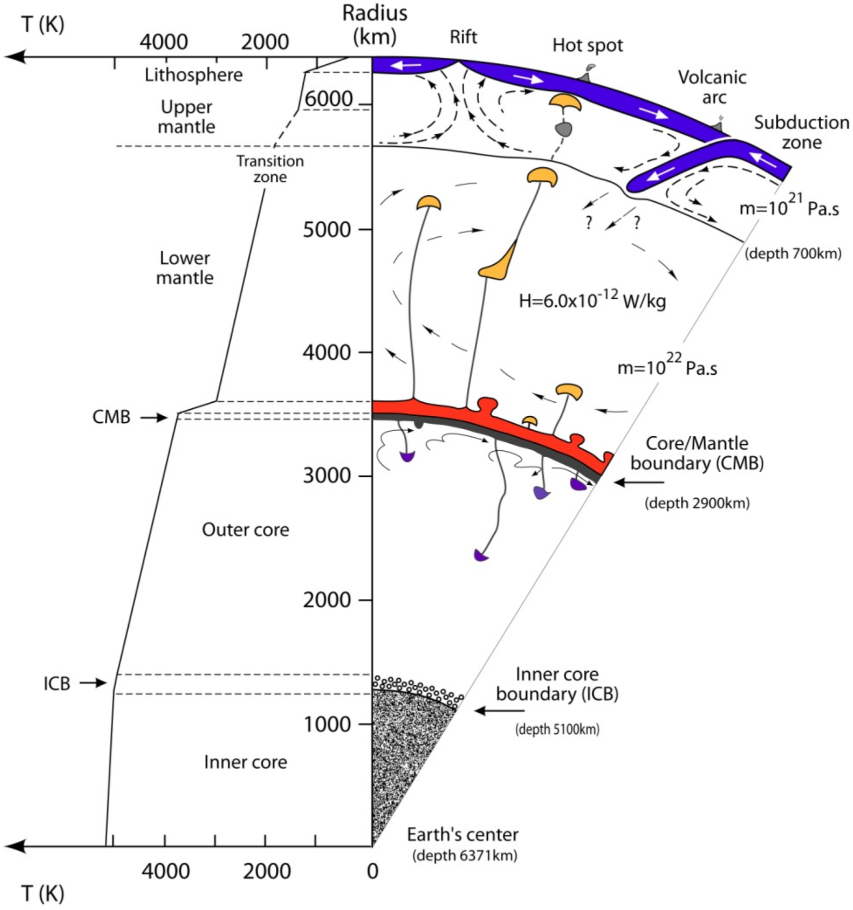

- Lateral structure?

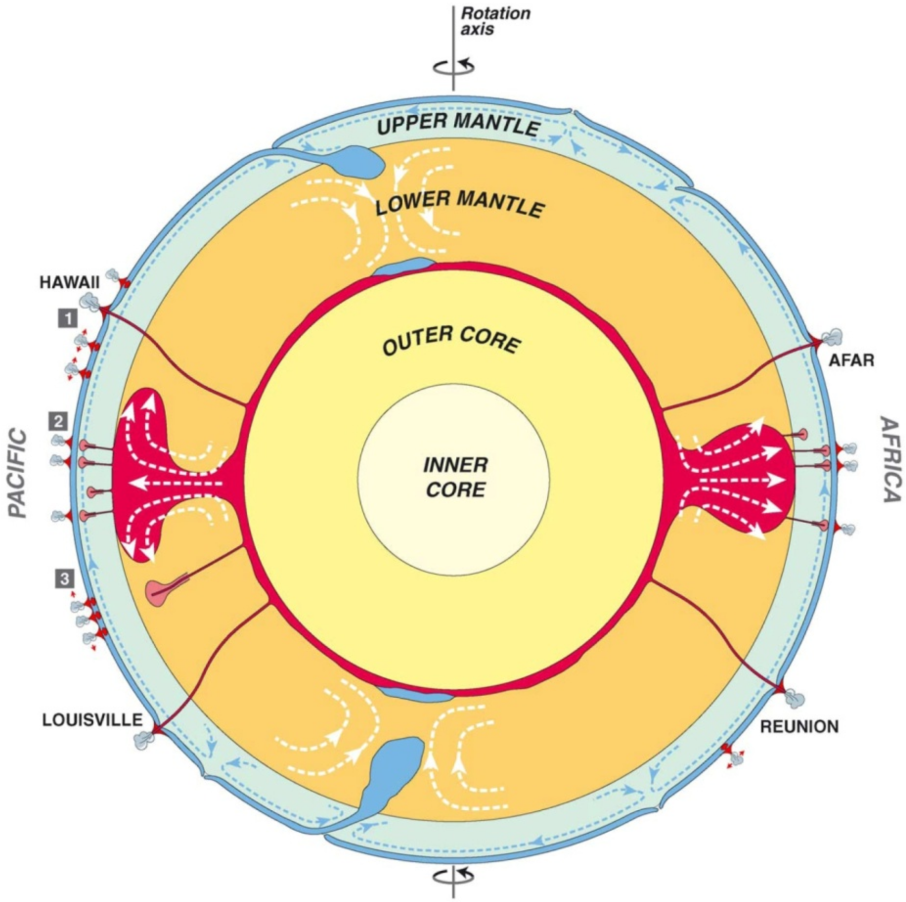

Courtillot et al. (2003)

Deep Earth 3D structure: recent views

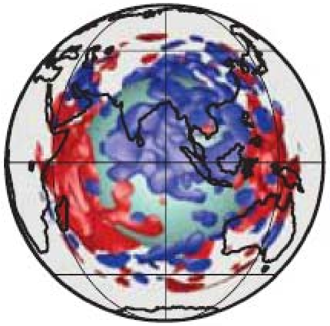

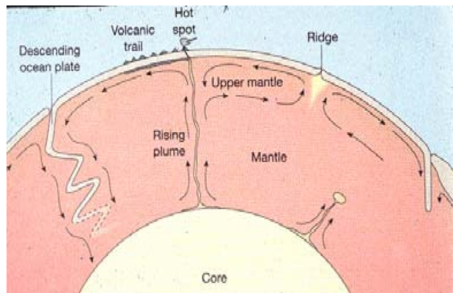

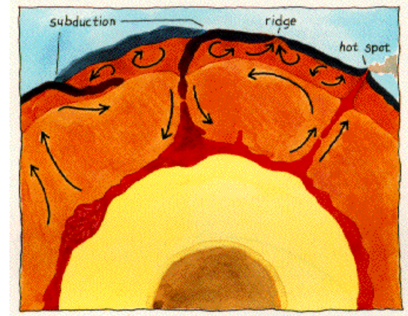

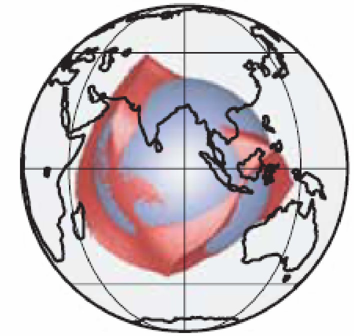

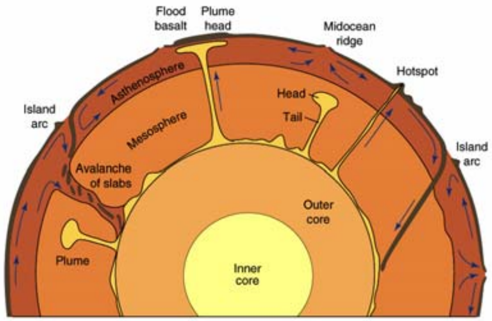

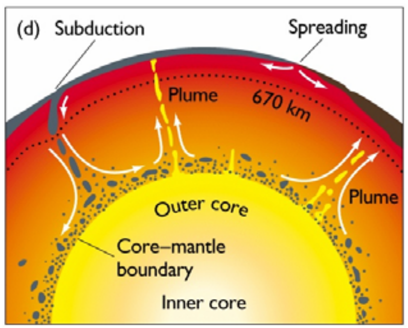

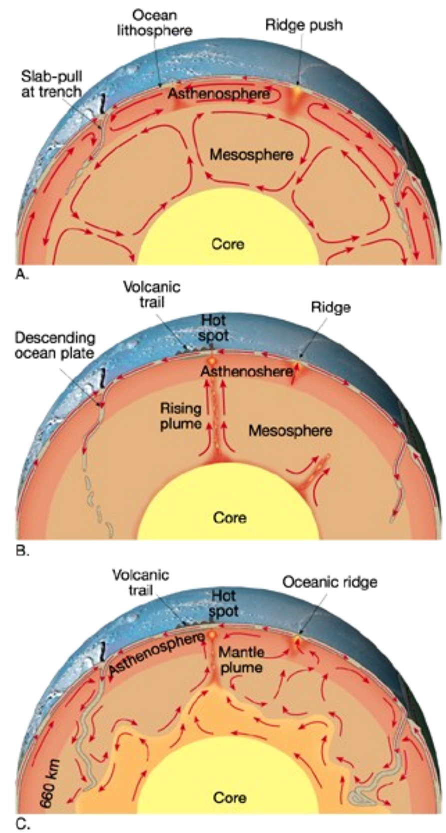

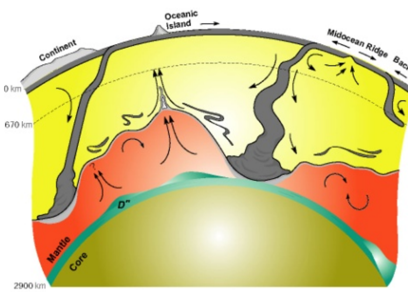

Kellogg, et al 19 MARCH 1999 VOL 283 SCIENCE

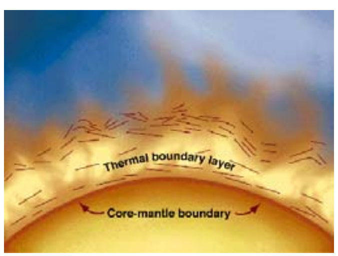

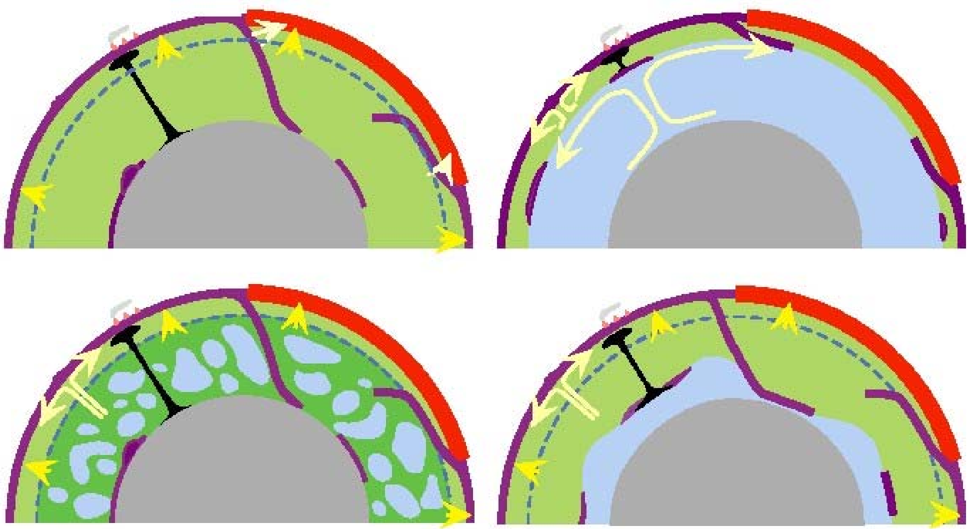

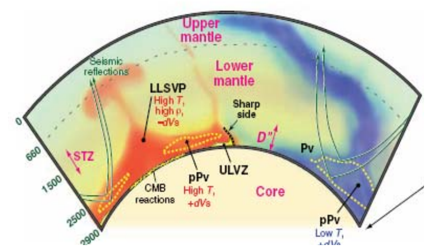

Geophysical constraints and models of mantle dynamics

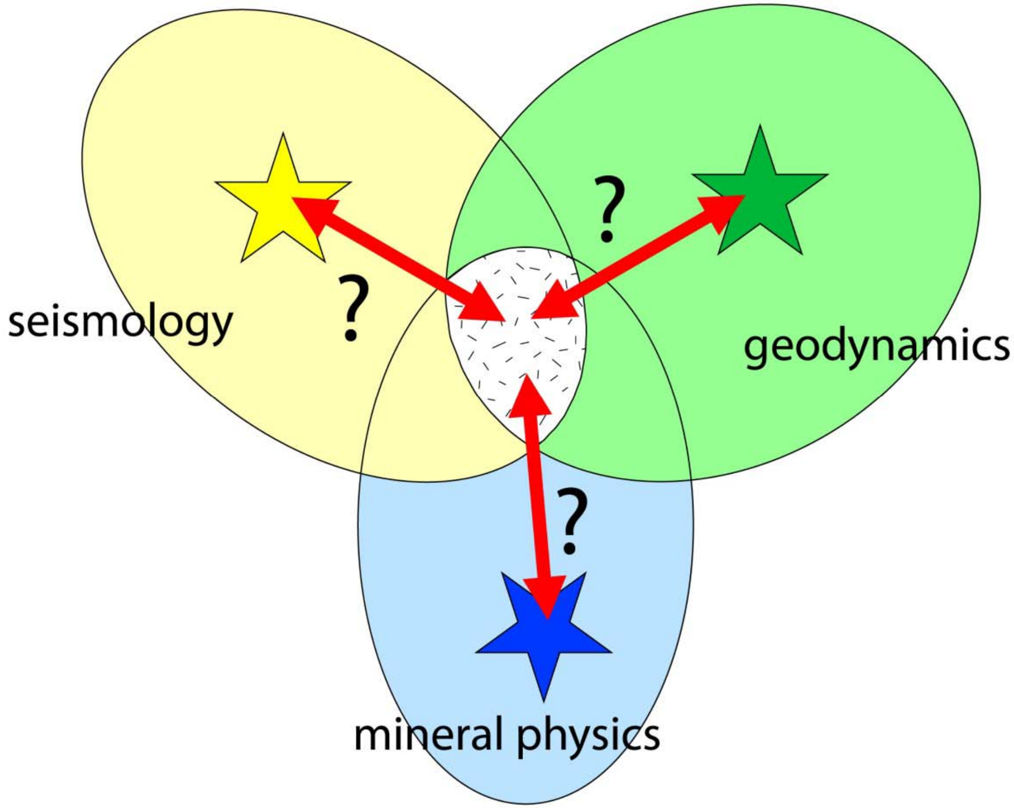

Can we find thermo-chemical structures that satisfy seismological observations, mineral physics data, and geodynamics models ?

Earth mantle: tomography and temperature

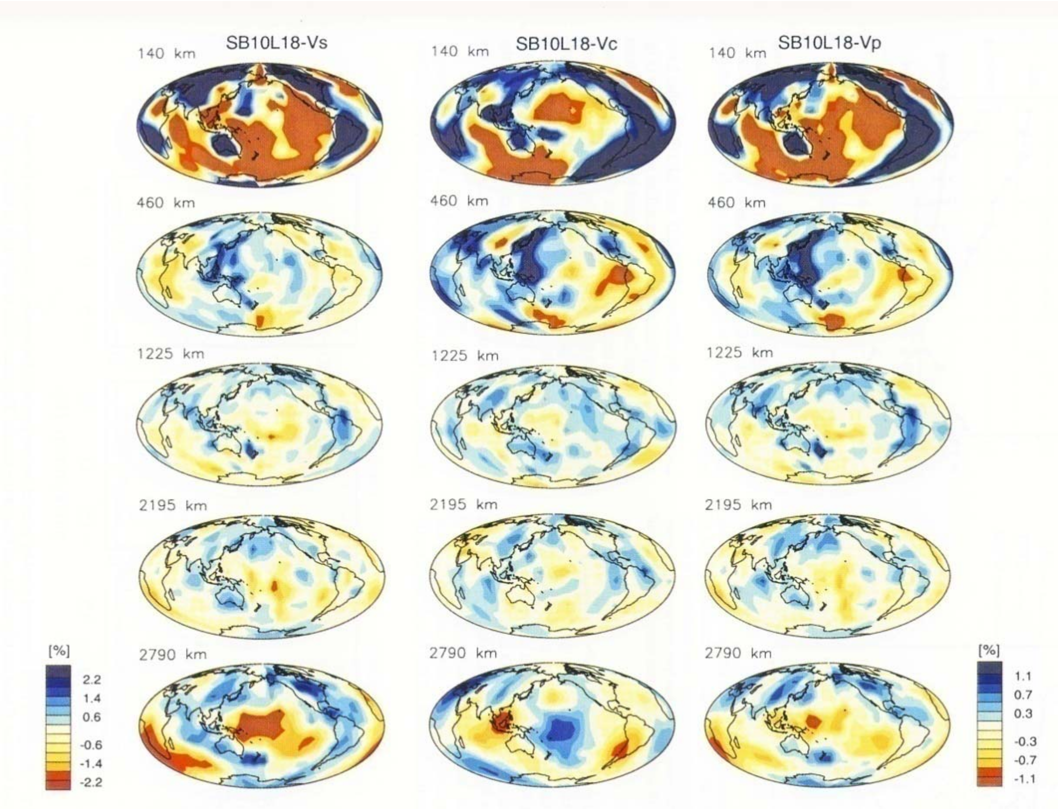

Masters et al. (2000)

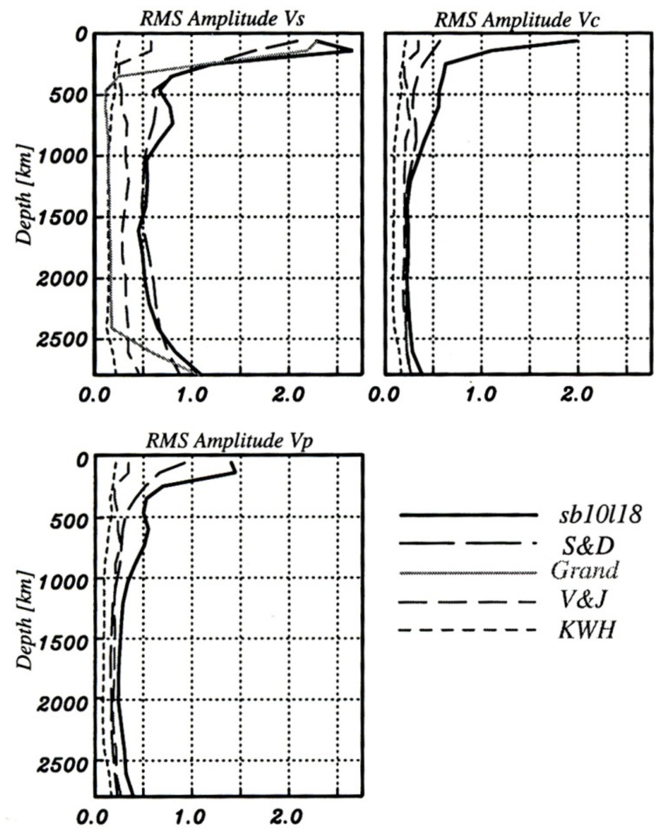

Seismic velocities decrease with increasing temperature, but are seismic velocity anomalies a good proxy for temperature anomalies?

Large low Shear-wave velocity provinces

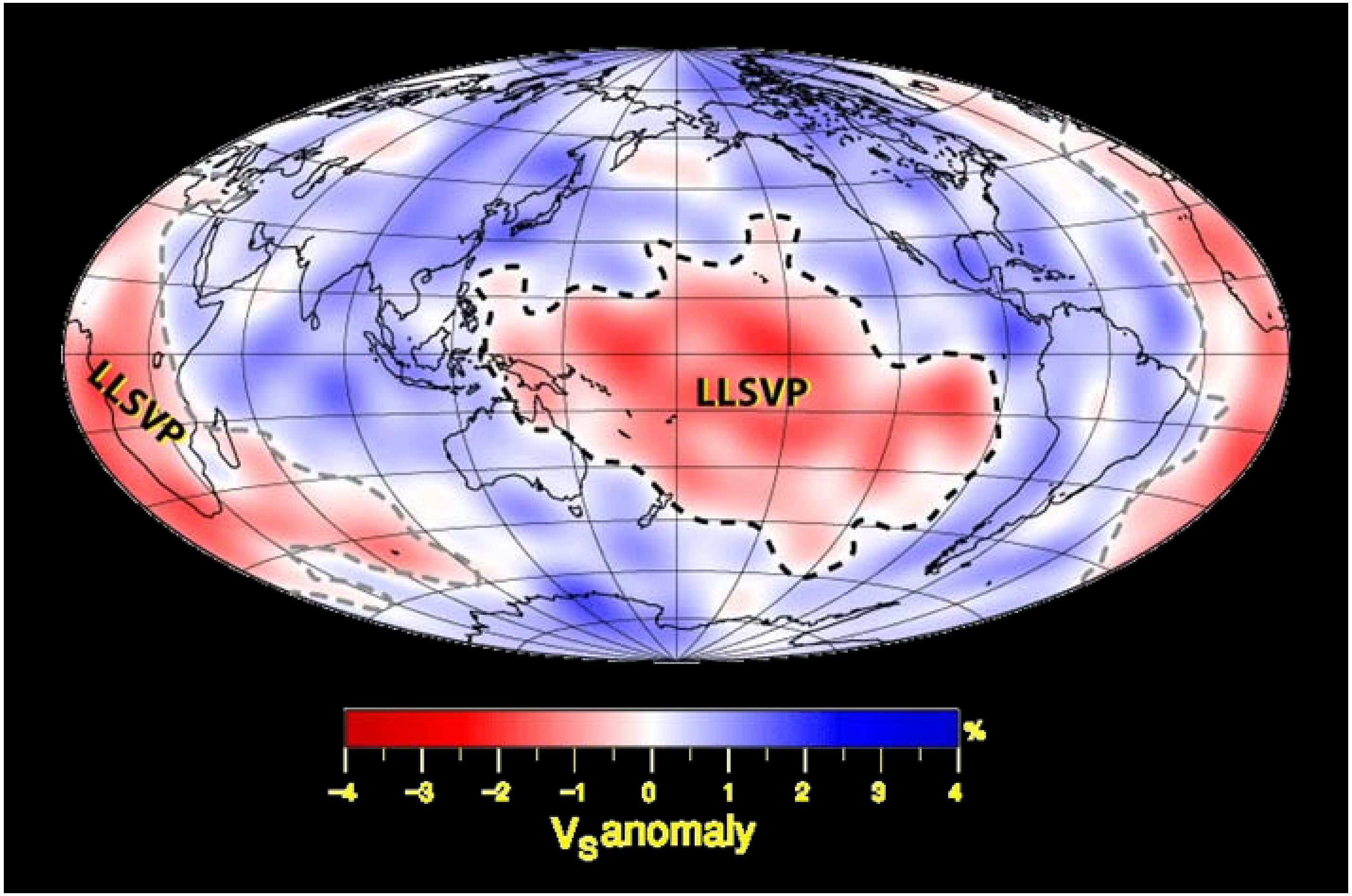

- Superplumes (= thermal) ?
- Recycled (heated) MORBs ?
- Primitive (chemically differentiated) reservoir ?

The fate of slabs: regional variations

Tomographic images shows that oceanic slabs have different fate depending on the region:

- Deflection and stacking around 700-1000 km *(Japan, Izu-Bonin)*.

- Sinking (avalanches) in the deep mantle *(Tonga, Central America)*.

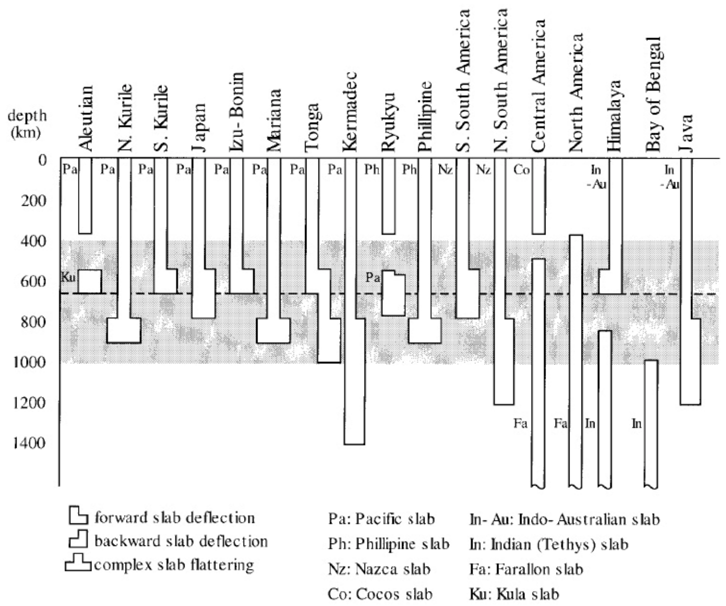

Fukao et al. (2001)

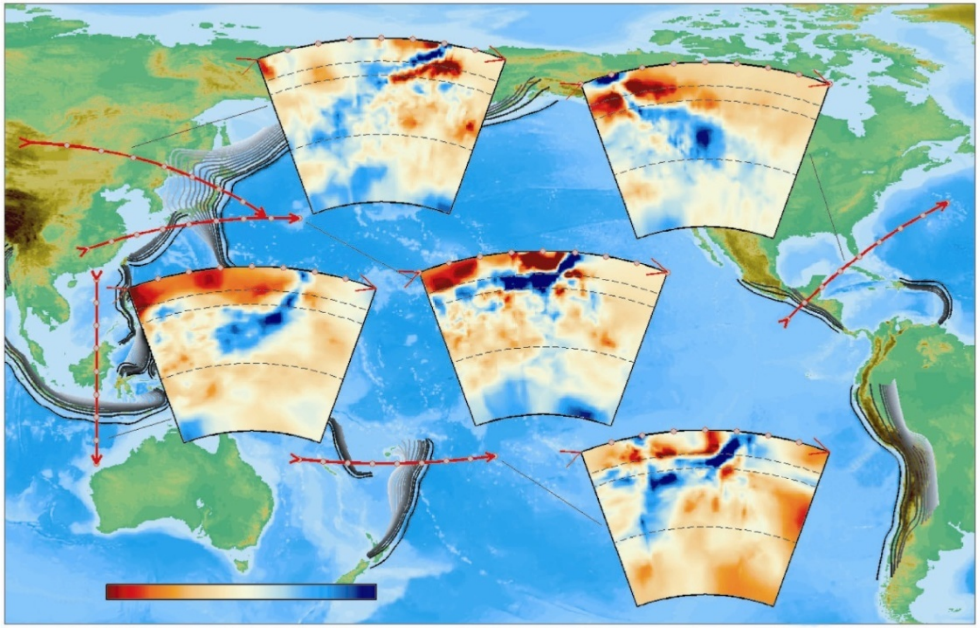

Kárason and van der Hilst (2000)

Plumes: observations

Finite frequency tomography: hotspots originate from various depths …

Lower mantle, CMB *Upper mantle*

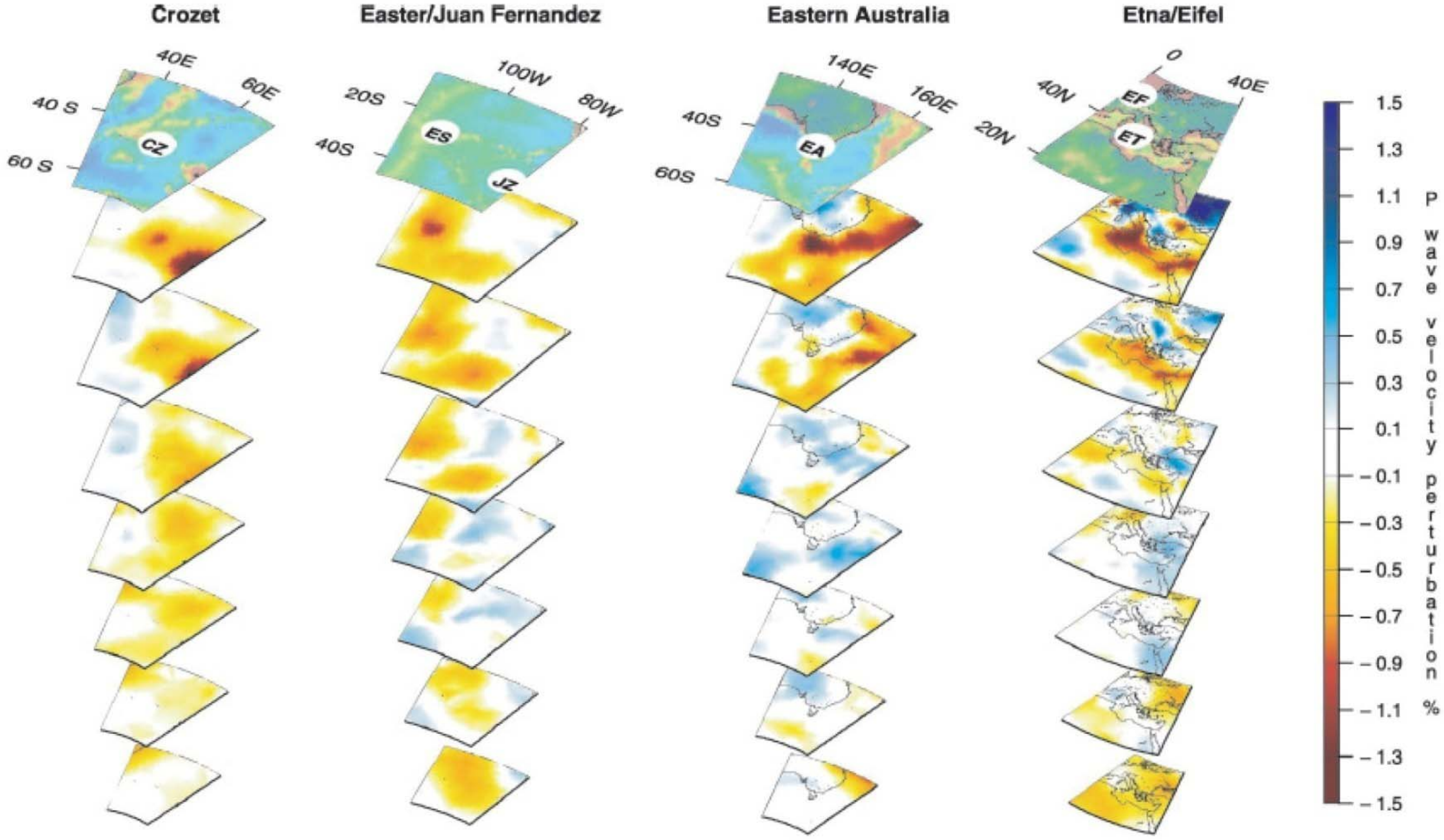

Montelli et al. (2004)

Earth's deep interior

- Connected to the surface through subduction (and plumes?).
- Mid-mantle shows little structure, but lower mantle highly heterogeneous (LLSVP, ULVZ).
- Nature and origin of heterogeneities (thermal, chemical, phase transition) ?

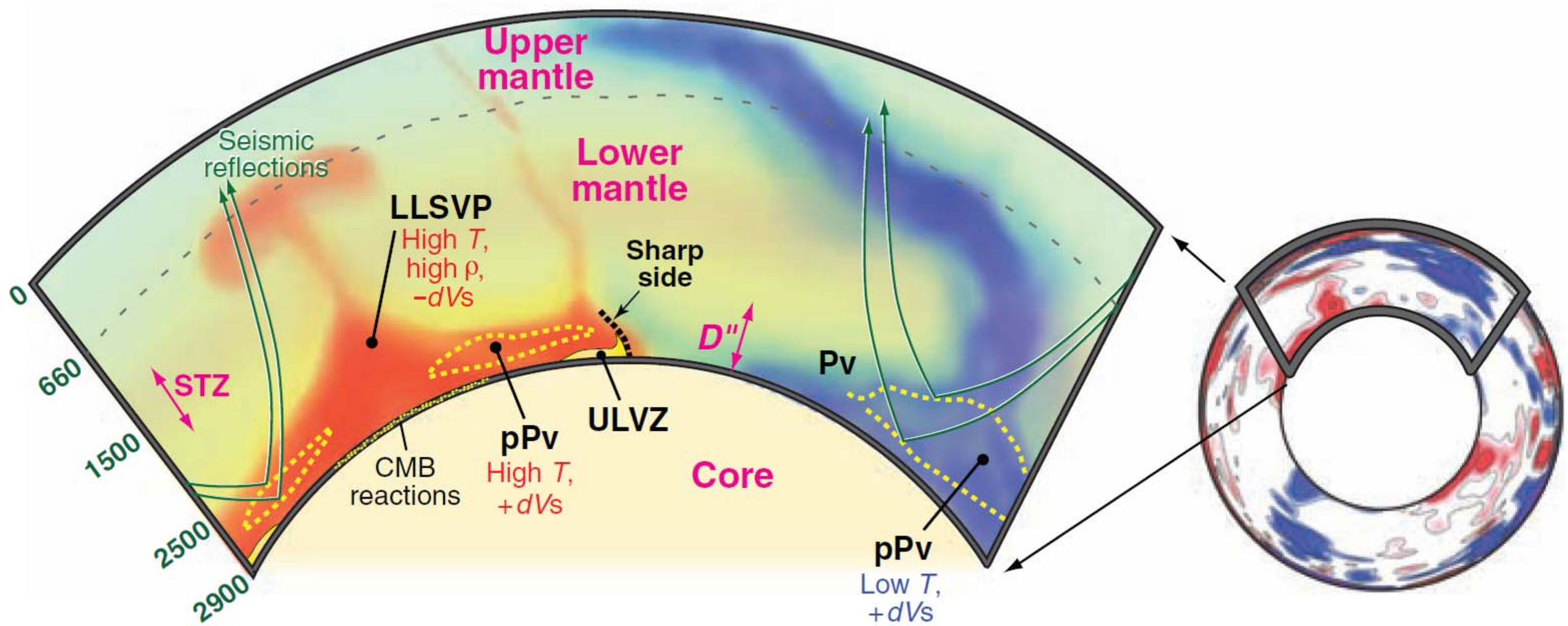

Garnero and McNamara (2008)

⇨ Strong compositional heterogeneities (that can be mapped by probabilistic tomography) are needed to explain seismic tomography anomalies.

⇨ Models of thermo-chemical convection that can maintain primitive reservoirs at the bottom of the mantle

Distributions of thermal and chemical anomalies in the lower mantle

- Seismology provides (so far) the best data to map the heterogeneities within the mantle.

- But how to interpret seismic velocity anomalies?

- Thermal and/or chemical?

- Thermo-elastic properties of mantle aggregate?

- Uncertainties and a priori *information?*

▶ Mineral physics data and Equation of State modeling.

▶ Density from normal modes to break trade-offs.

▶ Monte-Carlo search to explore the model space and estimate error bars.

Seismic ratios $d\ln V_\Phi/d\ln V_S$ and $d\ln V_S/d\ln V_P$

$d\ln V_\Phi/d\ln V_S$ increases with depth from 2000 km down to the CMB (*van der Hilst and Karàson*, 1999; *Masters et al.*, 2000).

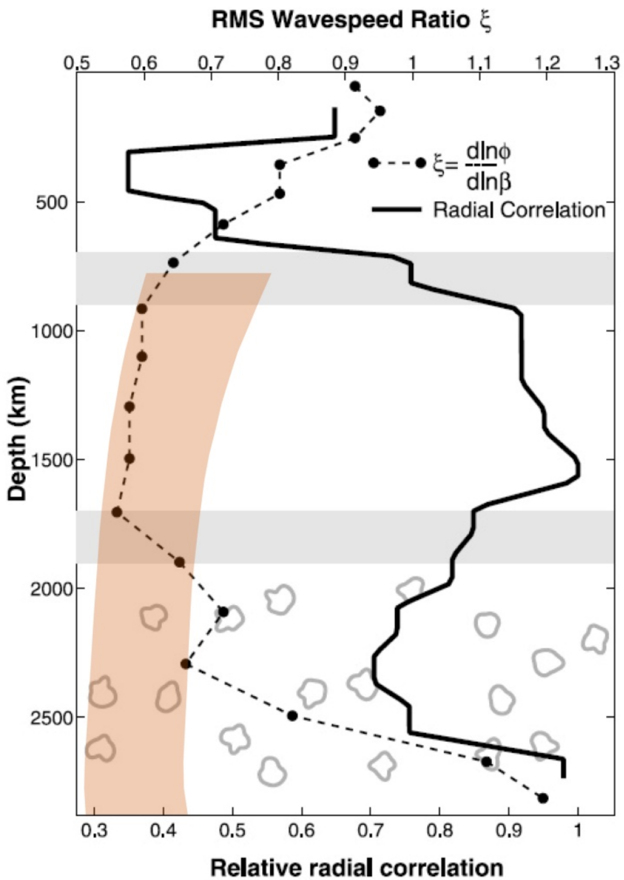

van der Hilst and Karàson (1999)

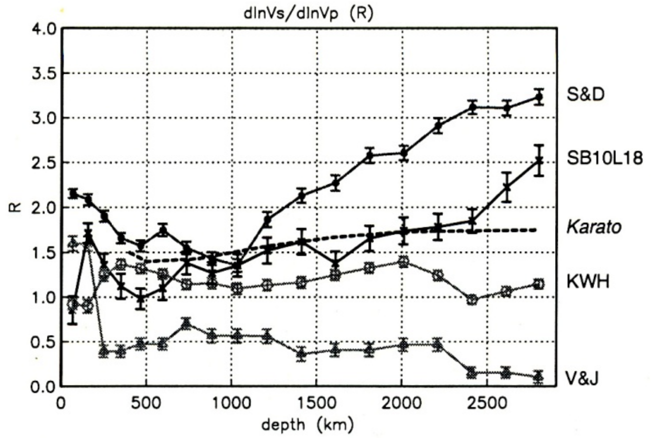

Masters et al. (2000)

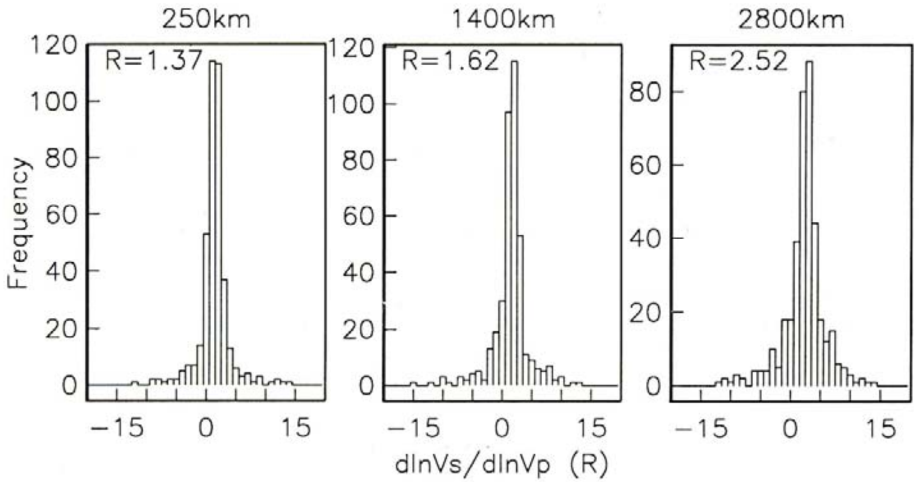

Masters et al. (2000)

Lateral distribution in the seismic ratio $d\ln V_S/d\ln V_P$

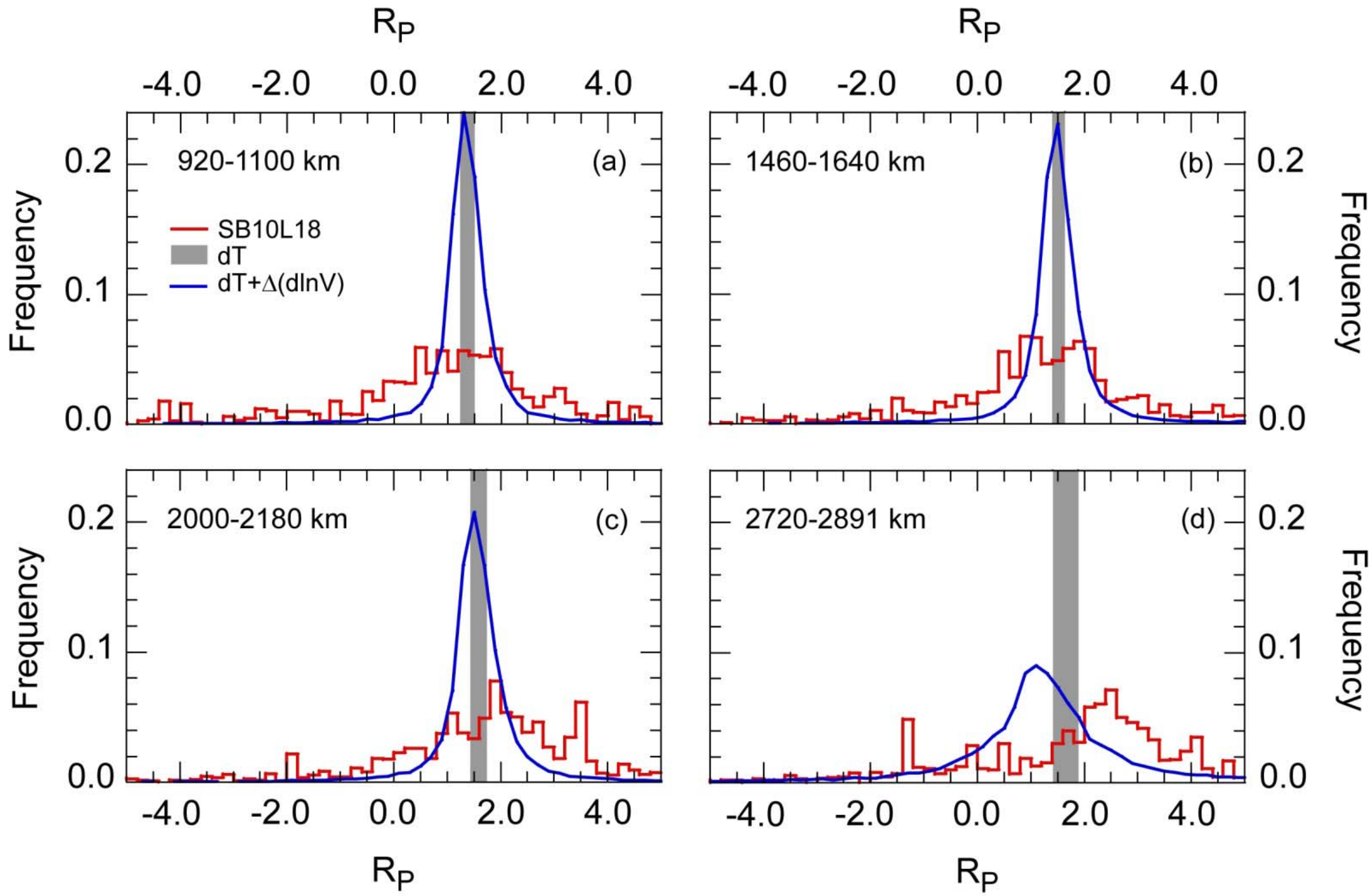

$R_P = d\ln V_S/d\ln V_P$

Deschamps and Trampert (2003)

The strong dispersion in the lateral distribution of the seismic ratio $d\ln V_S/d\ln V_P$, is incompatible with a purely thermal origin of seismic anomalies

Density & seismic velocities are not correlated

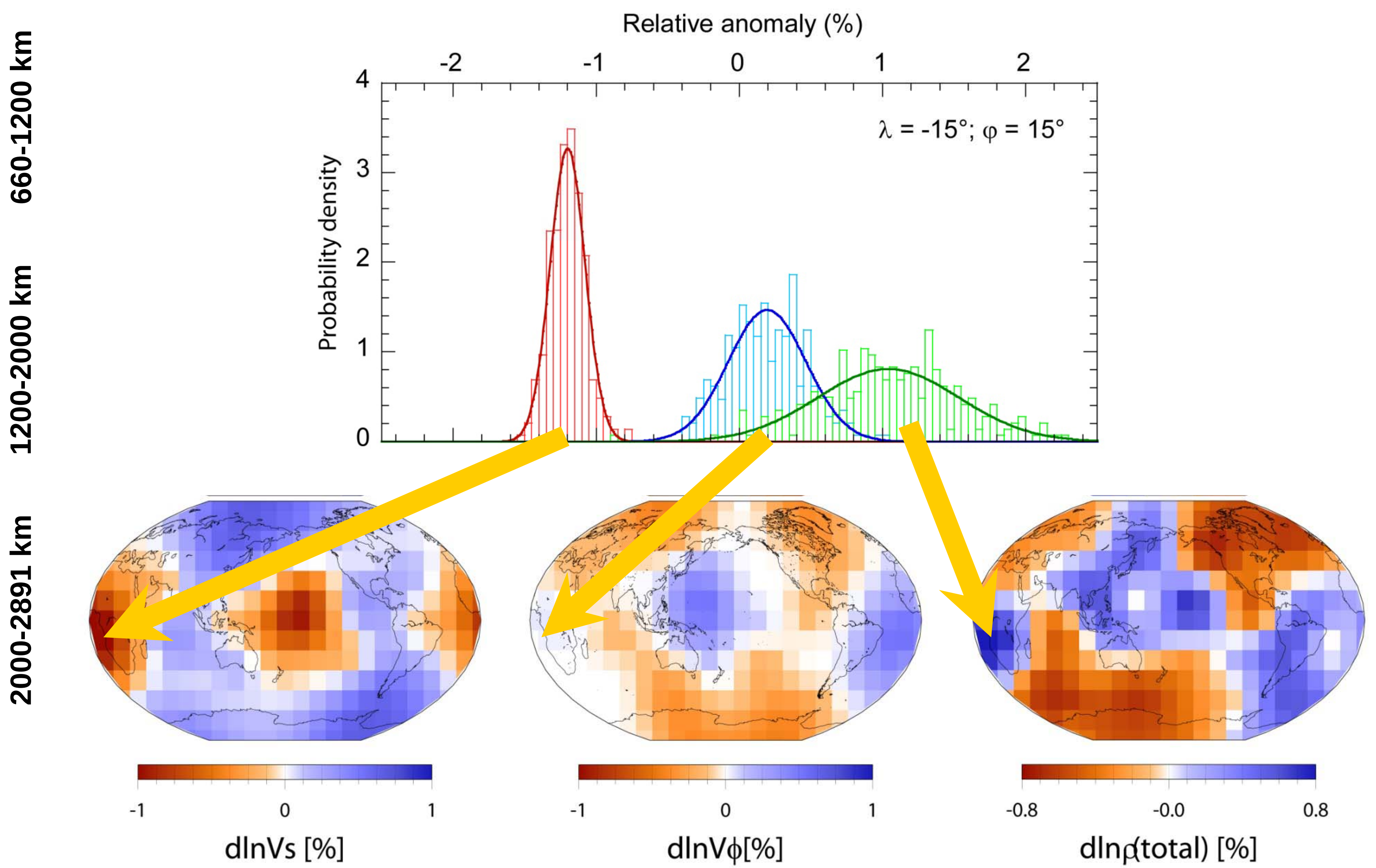

Probabilistic tomography (Trampert, Deschamps, Resovsky, & Yuen, 2004)

heterogeneieties

heterogeneities

- Two main minerals:

  - Perovskite, (Mg,Fe,Ca)SiO_3
  - Magnesio-wüstite, (Mg,Fe)O

Pyrolitic (=average) mantle: ~80% pv, with x_{Fe} ~12%.

⇨ *Perovskite vs magnesio-wüstite*

⇨ *Volume fraction of iron (FeO).*

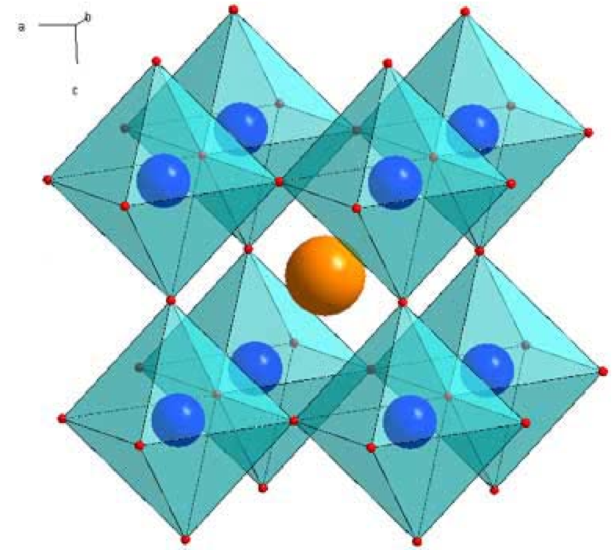

$CaTiO_3$ *perovskite structure*

- Stishovite (SiO_2) present in slabs.

⇨ *Volume of MORBs*

- Post-perovskite (*Murakami et al., 2004*; *Oganov and Ono, 2004*). Exothermic transition around 120 GPa (and 2500 K), with large Clapeyron slope (8-10 Mpa/K).

⇨ *Lateral variations in the topography of ppv*

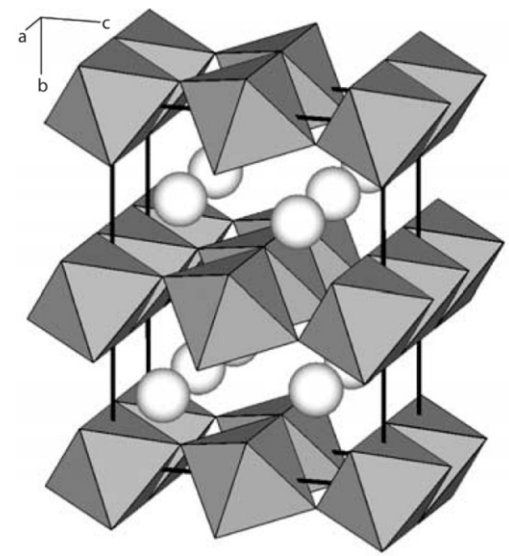

$CaTiO_3$ *post-perovskite structure*

From tomographic to thermo-chemical maps

- Anomalies in density and seismic velocities can be interpreted in terms of variations of temperature and composition *(e.g. volume fractions of iron and perovskite)*:

$$\begin{cases} d\ln V_S = \boxed{\dfrac{\partial \ln V_S}{\partial T}} dT + \boxed{\dfrac{\partial \ln V_S}{\partial x_{pv}}} dx_{pv} + \boxed{\dfrac{\partial \ln V_S}{\partial x_{Fe}}} dx_{Fe} \\ d\ln V_\Phi = \boxed{\dfrac{\partial \ln V_\Phi}{\partial T}} dT + \boxed{\dfrac{\partial \ln V_\Phi}{\partial x_{pv}}} dx_{pv} + \boxed{\dfrac{\partial \ln V_\Phi}{\partial x_{Fe}}} dx_{Fe} \\ d\ln \rho = \boxed{\dfrac{\partial \ln \rho}{\partial T}} dT + \boxed{\dfrac{\partial \ln \rho}{\partial x_{pv}}} dx_{pv} + \boxed{\dfrac{\partial \ln \rho}{\partial x_{Fe}}} dx_{Fe} \end{cases}$$

- Calculation of sensitivities needs thermo-elastic data and equation of state modeling *(thermo-elastic properties & density at high pressures & temperatures)*.

Equation of State modeling

- Thermo-elastic properties and density at high pressures and temperatures from thermo-elastic properties & density at $T = T_0$ and $P = 0$

- For each mineral of the aggregate:

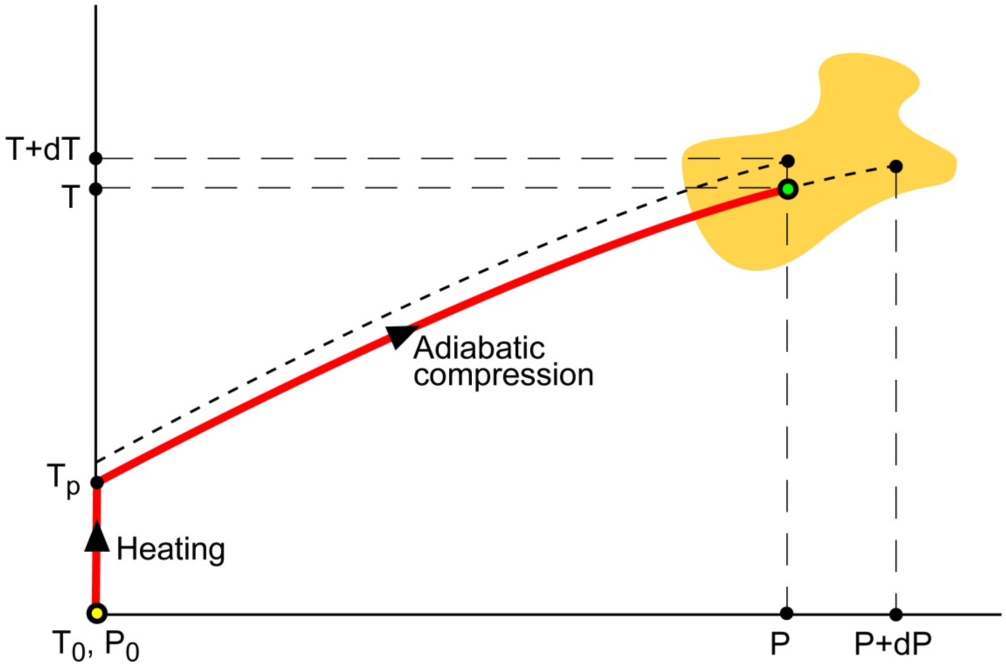

- High temperature extrapolation:

$$\rho(T_p, P=0) = \rho_0 \exp\left[-\int_{T_0}^{T_p} \alpha(T)\,dT\right]$$

$$K_S(T_p, P=0) = K_{S0} \exp\left[\frac{\rho(T_p, P=0)}{\rho_0}\right]^{\delta_{S_0}}$$

- High pressure extrapolation (Birch-Murnaghan to 3rd order):

$$P = -3K_{S0}(1-2\varepsilon)^{5/2}\left[\varepsilon + \frac{3}{2}(4 - K'_{S0})\varepsilon^2\right]$$

$$\rho(T,P) = \rho(T, P=0)(1-2\varepsilon)^{3/2}$$

$$K_S = K_{S0}(1-2\varepsilon)^{5/2} \times \left[1 + (5 - 3K'_{S0})\varepsilon - \frac{27}{2}(4 - K'_{S0})\varepsilon^2\right]$$

- Uncertainties from error bars at $T = T_0$ and $P = 0$, and a Monte-Carlo Search.

- Thermo-elastic properties of the aggregate from Voigt-Reuss-Hill average.

Seismic sensitivities to temperature & Composition

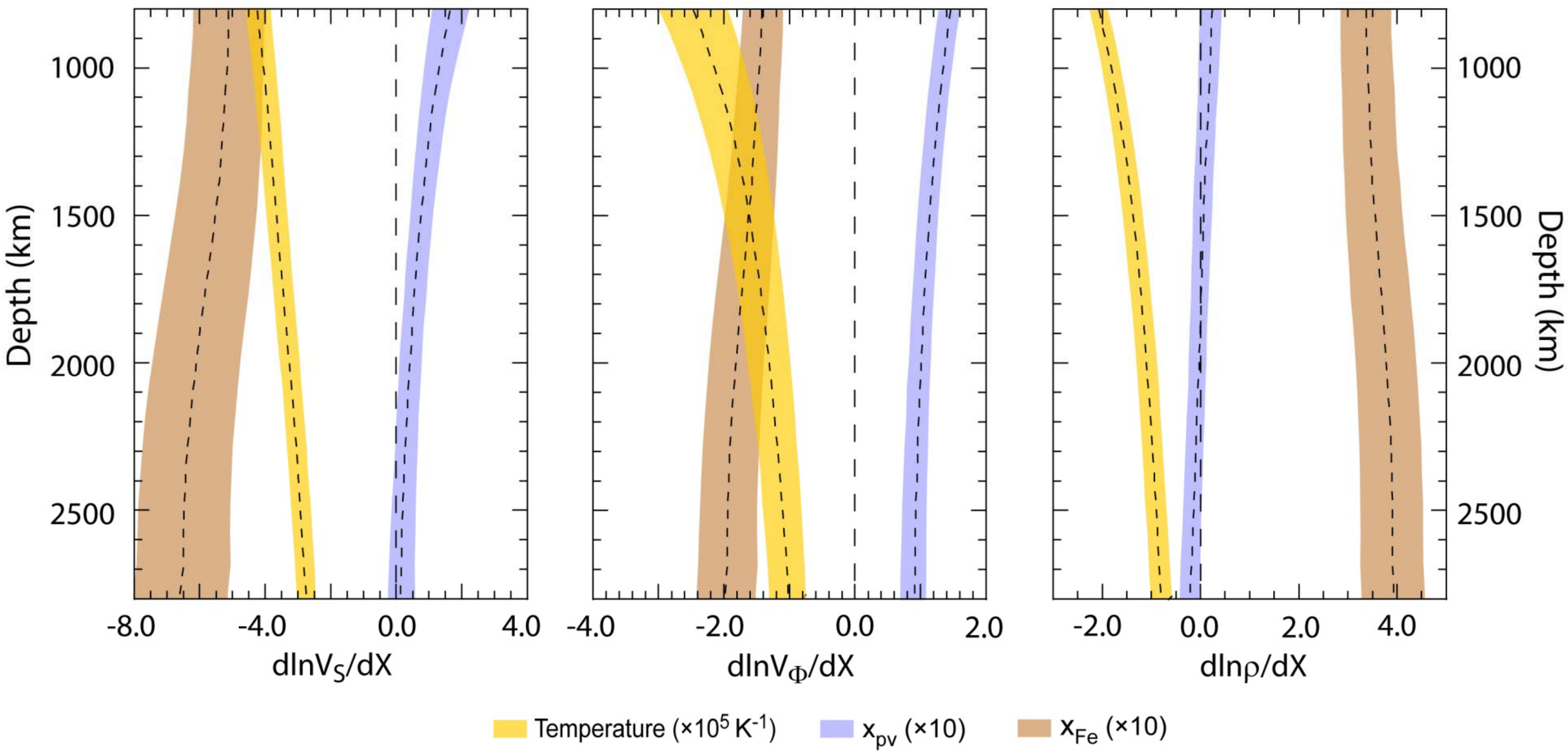

Deschamps and Trampert (2003); Deschamps et al. (2007)

- Shear-wave velocity and density are not sensitive to perovskite in the deep mantle
- Shear-wave velocity is sensitive to both temperature and iron throughout the mantle
- Density is mostly sensitive to iron in the deep mantle

Thermo-chemical structure from classical tomography

Deterministic inversions of dlnV_S and dlnV_P from SB10L18 (*Masters et al.*, 2000) (+ *a priori* random errors) for anomalies in temperature and perovskite.

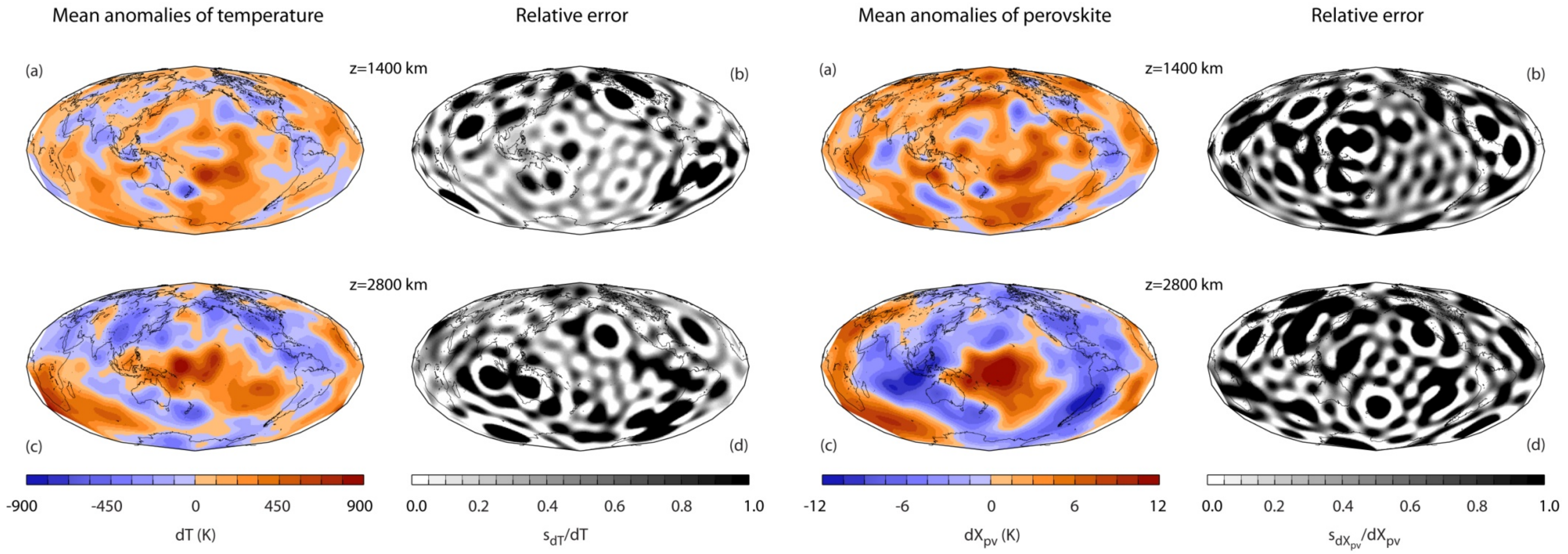

Deschamps and Trampert (2003)

For relative errors on velocity is higher than 0.3, composition is totally unconstrained, and temperature contain at least 50% errors

Deterministic inversions of velocity anomalies alone are not robust

Thermo-chemical structure from probabilistic tomography

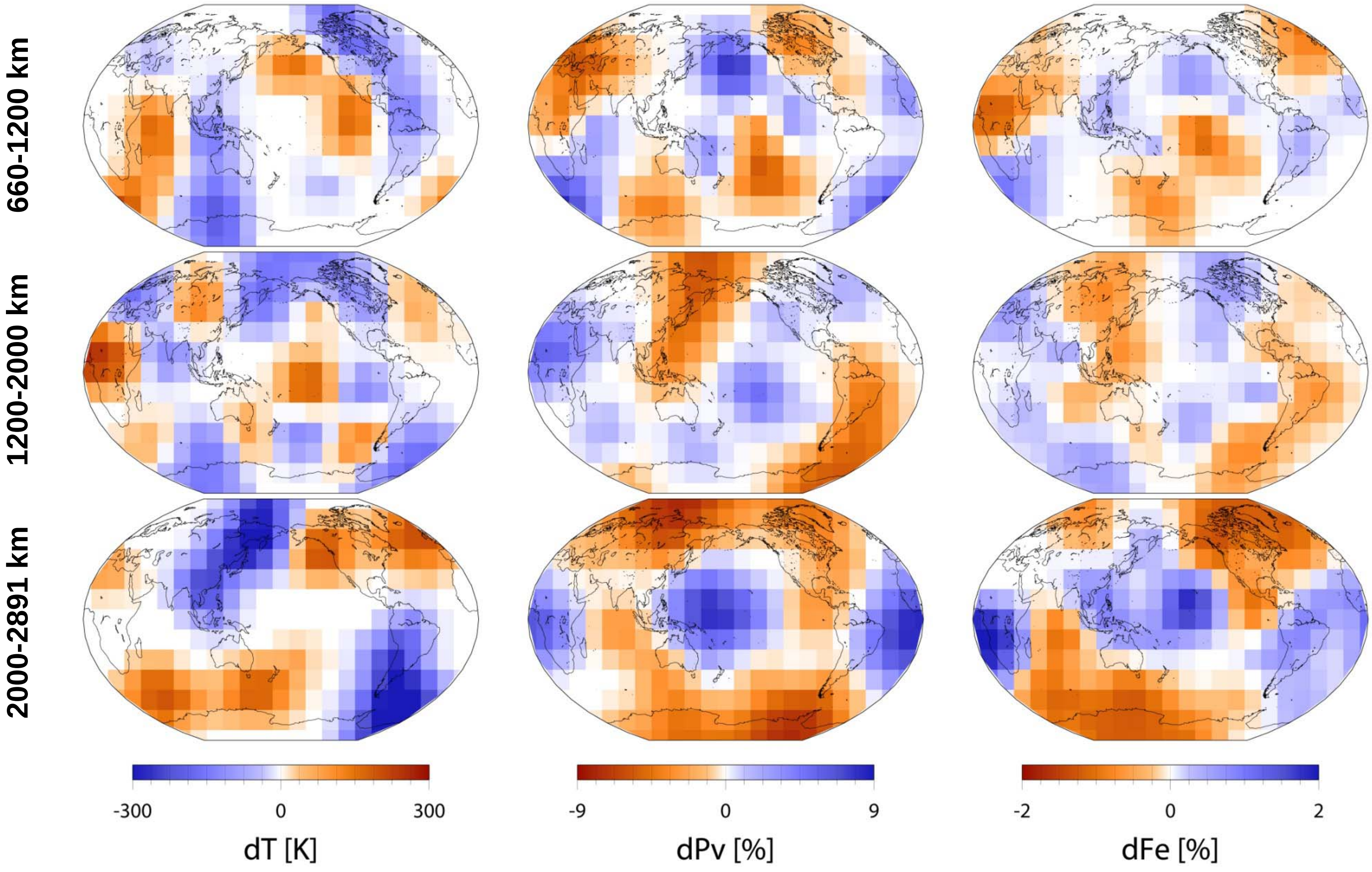

Trampert, Deschamps, Resovsky, & Yuen (2004)

Who sees what?

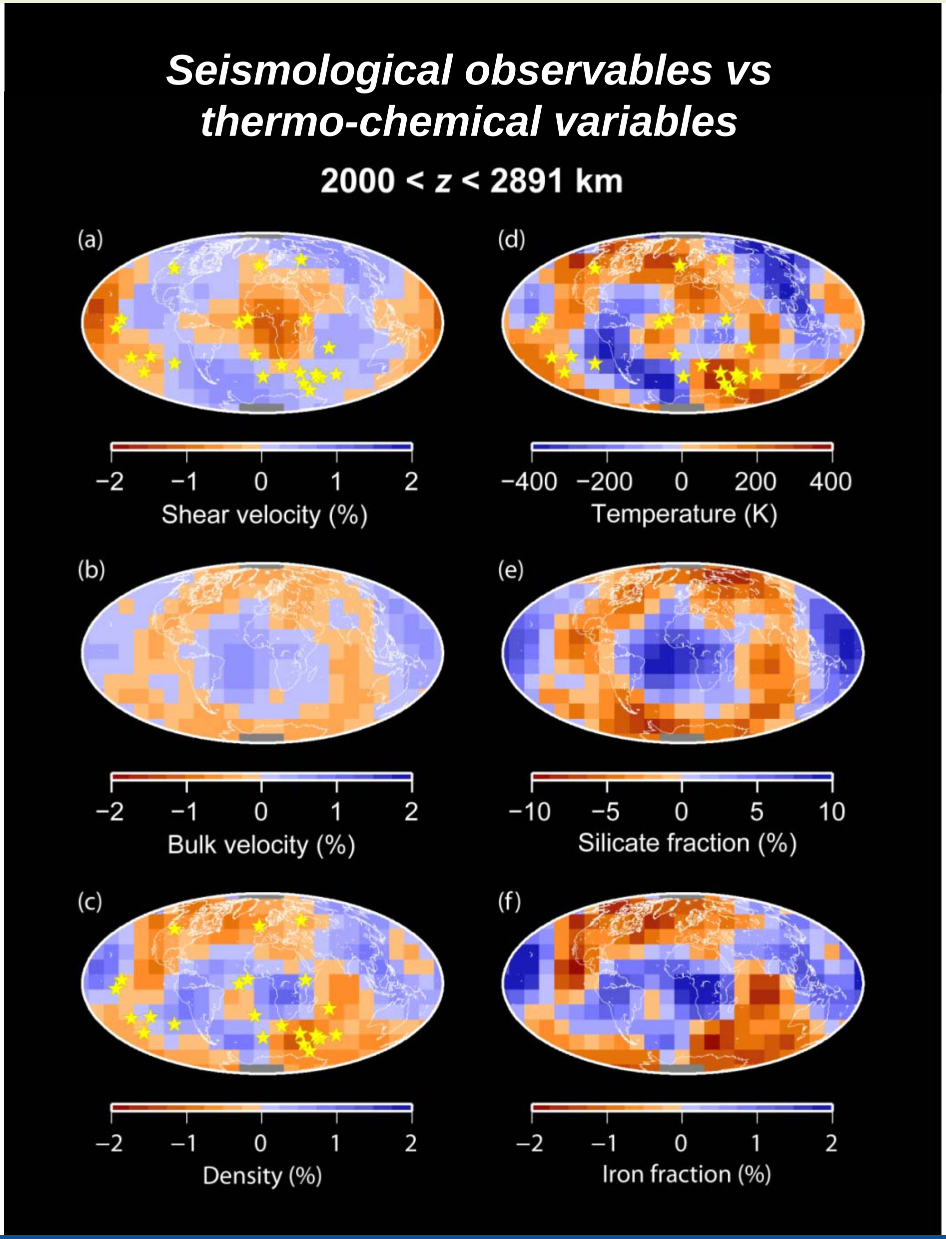

What is the mode of mantle convection?

● Thermo-chemical convection is essential to explain seismological observations.

● Some important remaining questions:

- What are the controlling parameters of thermo-chemical convection?

- Which model(s) explain observables (in particular from seismology)?

- How to maintain strong chemical heterogeneities (that survive convection) in the deep mantle?

▶ Numerical modeling using STAG3D (*Tackley*, 1998) and parallel calculations on a Linux cluster.

- Survival of primitive reservoirs at the bottom of the mantle.

- Influence of slab recycling

▶ Comparison with seismic tomography (in particular thermo-chemical distributions from probabilistic tomography, *Trampert et al.*, 2004).

Experimental thermo-chemical convection

- Evolution of a dense basal layer.
- Two modes, depending on the density contrast:
  - *- Stratification*
  - *- Oscillating domes*

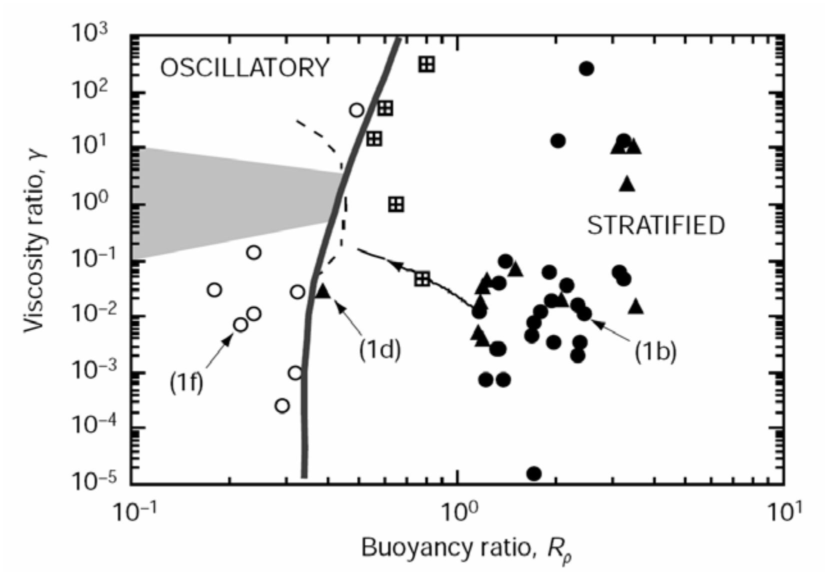

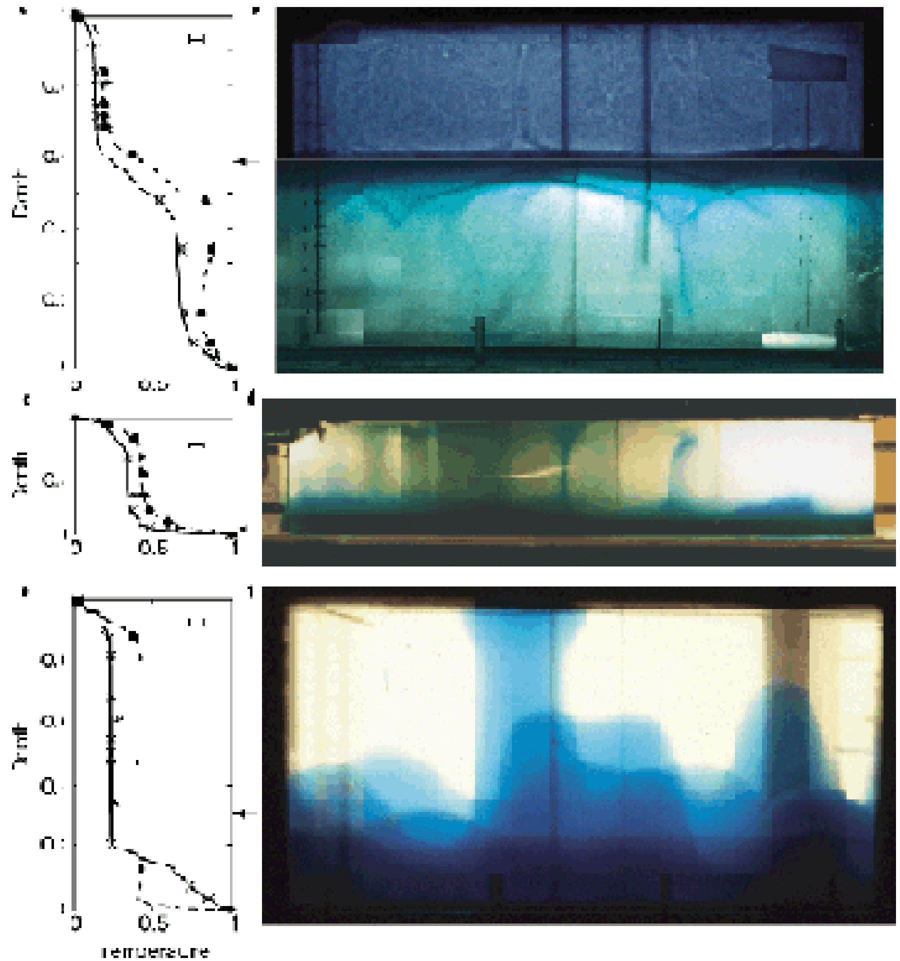

Davaille (1999)

Numerical thermo-chemical convection *(STAGYY)*

Solve the non-dimensional conservative equations of mass, momentum, energy, and composition for an anelastic, compressible fluid with an infinite Prandtl number:

$$\nabla \cdot (\rho \underline{u}) = 0$$

$$\nabla \cdot \underline{\underline{\sigma}} - \nabla P = Ra(\alpha \rho T - BC)\underline{e_z}$$

$$\rho C_p \frac{\partial T}{\partial t} = \nabla \cdot (k \nabla T) - \rho C_p \underline{u} \cdot \nabla T + \rho H - Di_s \alpha \rho T u_z + \frac{Di_s}{Ra} \sigma_{ij} \frac{\partial u_i}{\partial x_j}$$

$$\frac{\partial C}{\partial t} = -\underline{u} \cdot \nabla C$$

$$\sigma_{ij} = \eta \left(\frac{\partial u_i}{\partial x_j} + \frac{\partial u_j}{\partial x_i} - \frac{2}{3} \delta_{ij} \frac{\partial u_k}{\partial x_k} \right)$$

$$Ra = \frac{\alpha \rho g \Delta T_{sa} b^3}{\eta \kappa} \qquad B = \frac{\Delta \rho_c}{\alpha \rho \Delta T_{sa}}$$

Need computational ressources !

Reservoirs of primitive material

- How to maintain reservoirs of dense primitive material in the deep mantle?

▶ Extensive search in the model space of thermo-chemical convection, using STAG3D:

- Viscosity is temperature-, depth-, and compositional-dependent.

- 3D-Cartesian grid of 128×128×64 points *(+ a few runs on 128×384×64×2 Yin-Yang grids)*, and 12 tracers per grid.

- Two types of tracers (dense & regular material), with buoyancy ratio *B*. Dense tracers are initially distributed in a basal, dense layer. Compositional field is modeled by the distribution in the concentration in dense particles *C*.

- Explored parameters:

    * Rheology: thermal viscosity contrast, chemical viscosity contrast, depth variations

    * Buoyancy ratio (chemical density contrast).

    * Clapeyron slope of the phase transition at 660 km.

    * Volume fraction of dense material, mode of heating, …

Large buoyancy ratio: stable layering

Large buoyancy ratio (> 0.25, i.e. $\Delta\rho \sim 100$ kg/m^3):

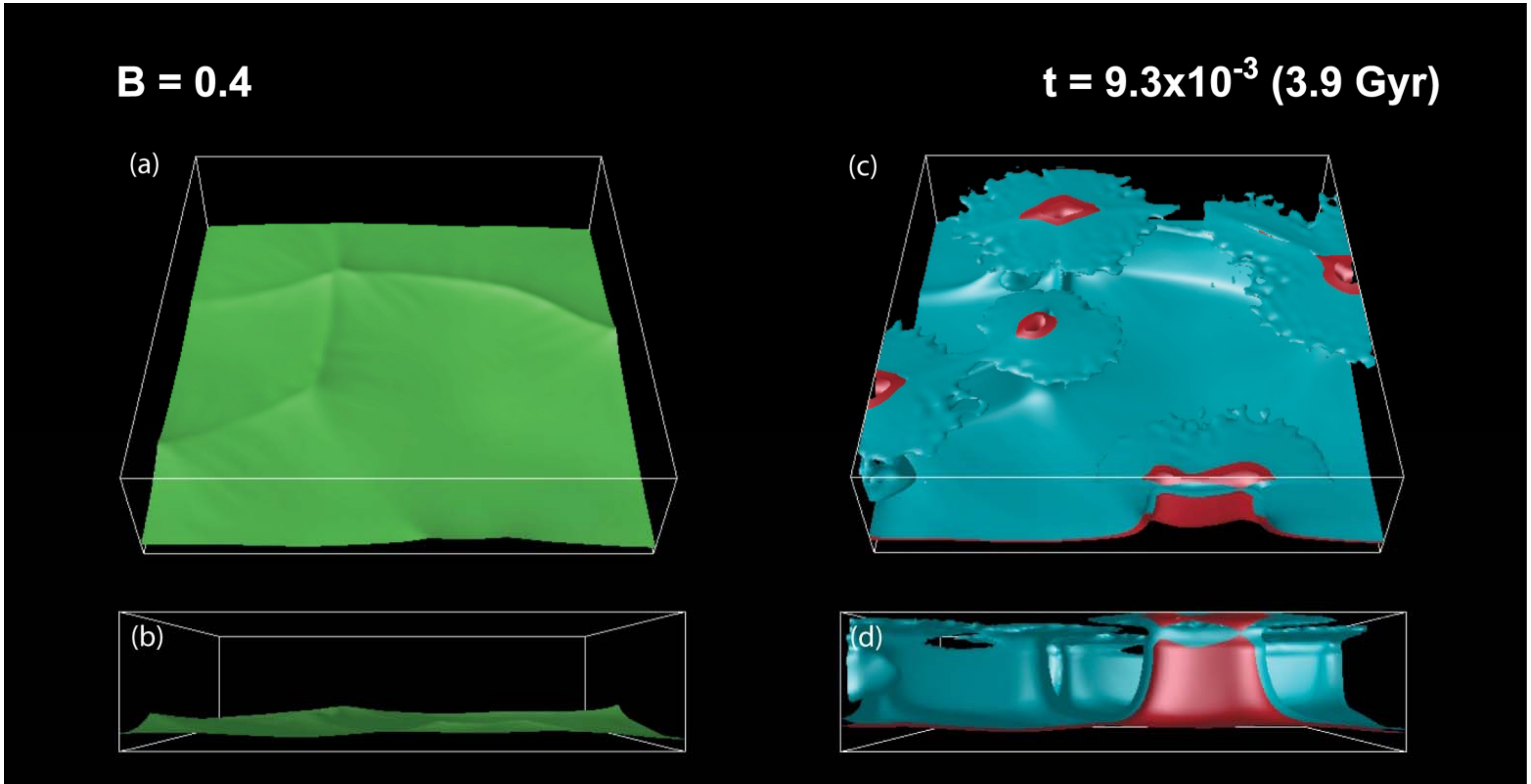

Isosurfaces of concentration in dense particles (left, C = 0.5), and residual temperature (right, blue is cold, red is hot) (Deschamps and Tackley, 2009).

Stable layering, inconsistent with tomography maps)

- Chemical stratification induces strong compositional anomalies at the limit between the dense and regular layers …
- … but the rest of the system is homogeneous.
- Inconsistent with seismic data and models.

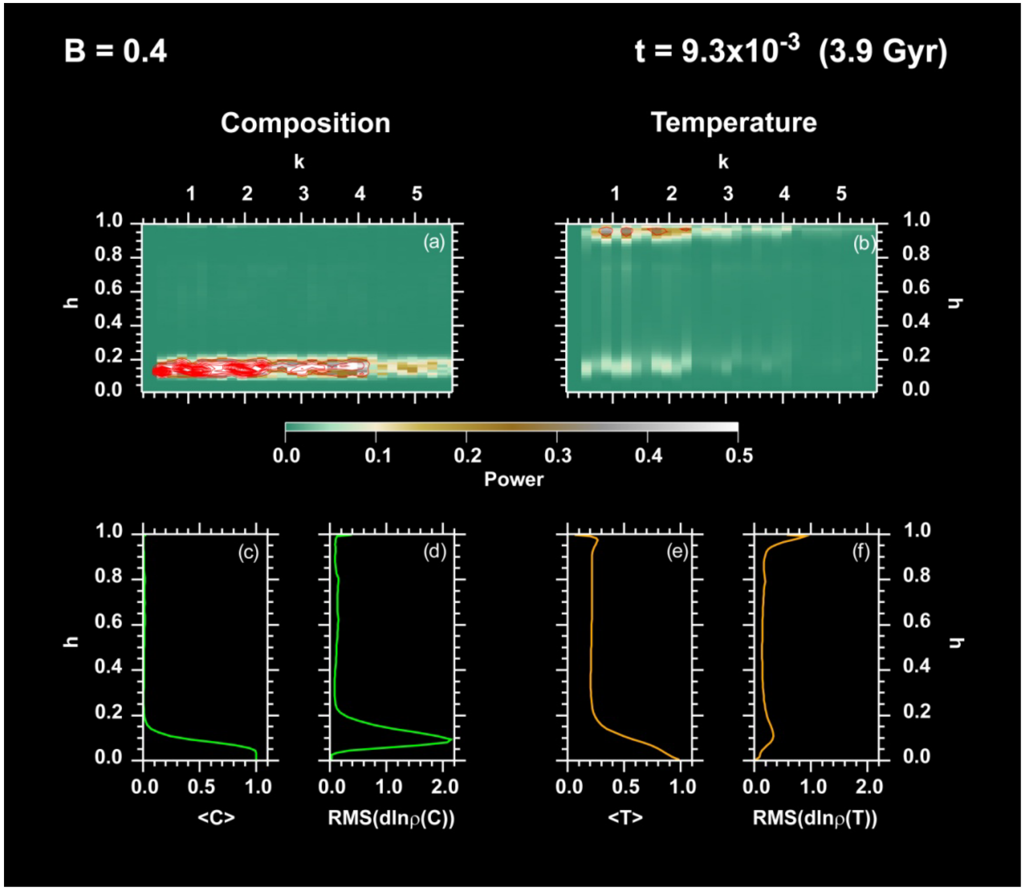

Moderate buoyancy ratio

Moderate buoyancy ratio (~ 0.20, i.e. $\Delta\rho$ ~ 80 kg/m³):

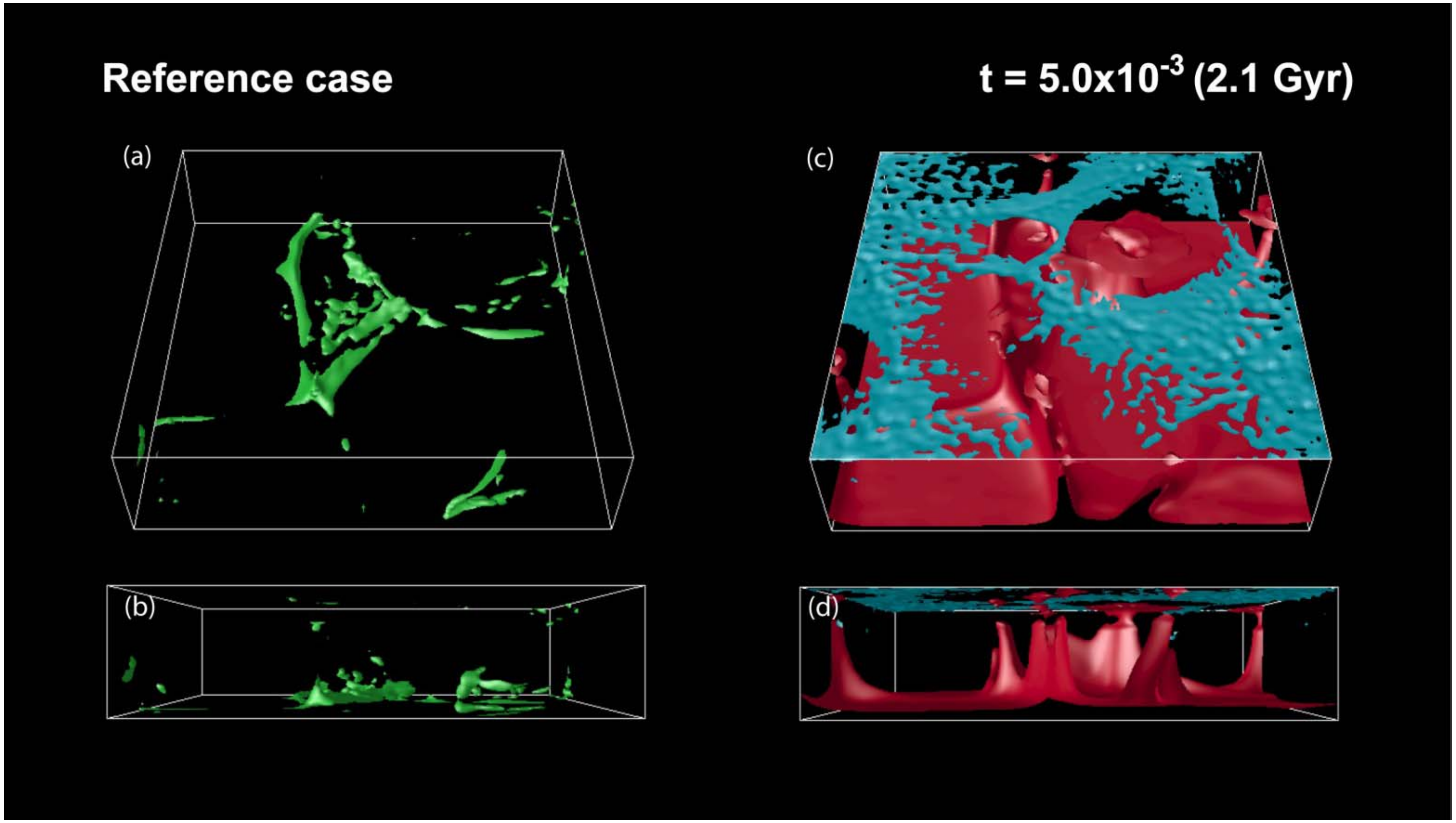

- Large thermo-chemical plumes are generated early in the calculation.
- But these structures are short-lived. Mixing is efficient and reservoirs of dense material cannot be maintained at the bottom of the system.

Thermal viscosity contrast

Large thermal viscosity contrast (10^4 and more):

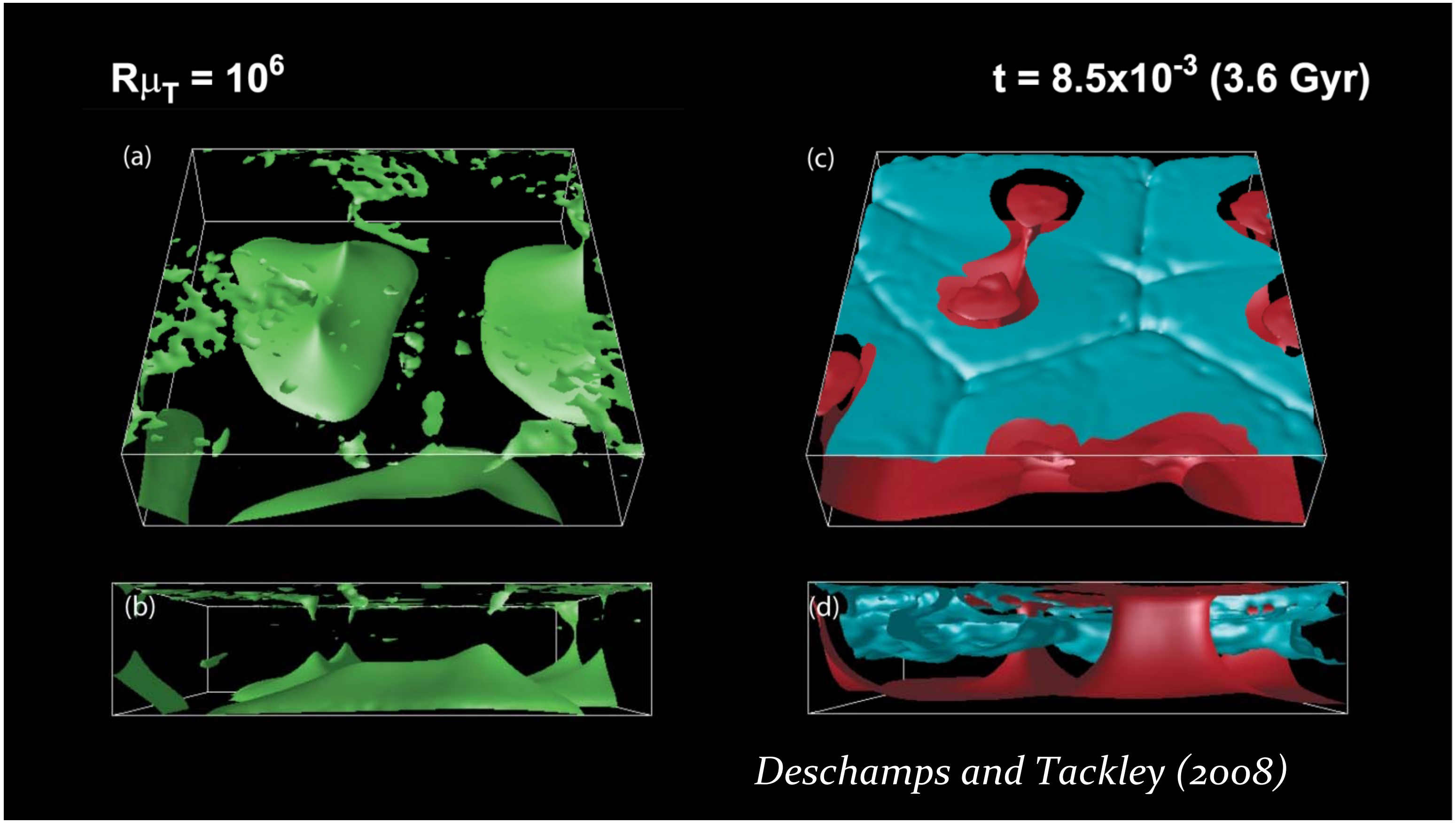

Large pools of dense material are generated at the bottom of the system and survive for a long period of time.

Thermal viscosity contrast
(*Profiles & spectral heterogeneity maps*)

- The chemical structure is dominated by strong compositional anomalies at the bottom (*h* < 0.2) of the system.

- The thermal structure is dominated by strong thermal anomalies below the surface ....

… and moderate anomalies at the bottom of the system.

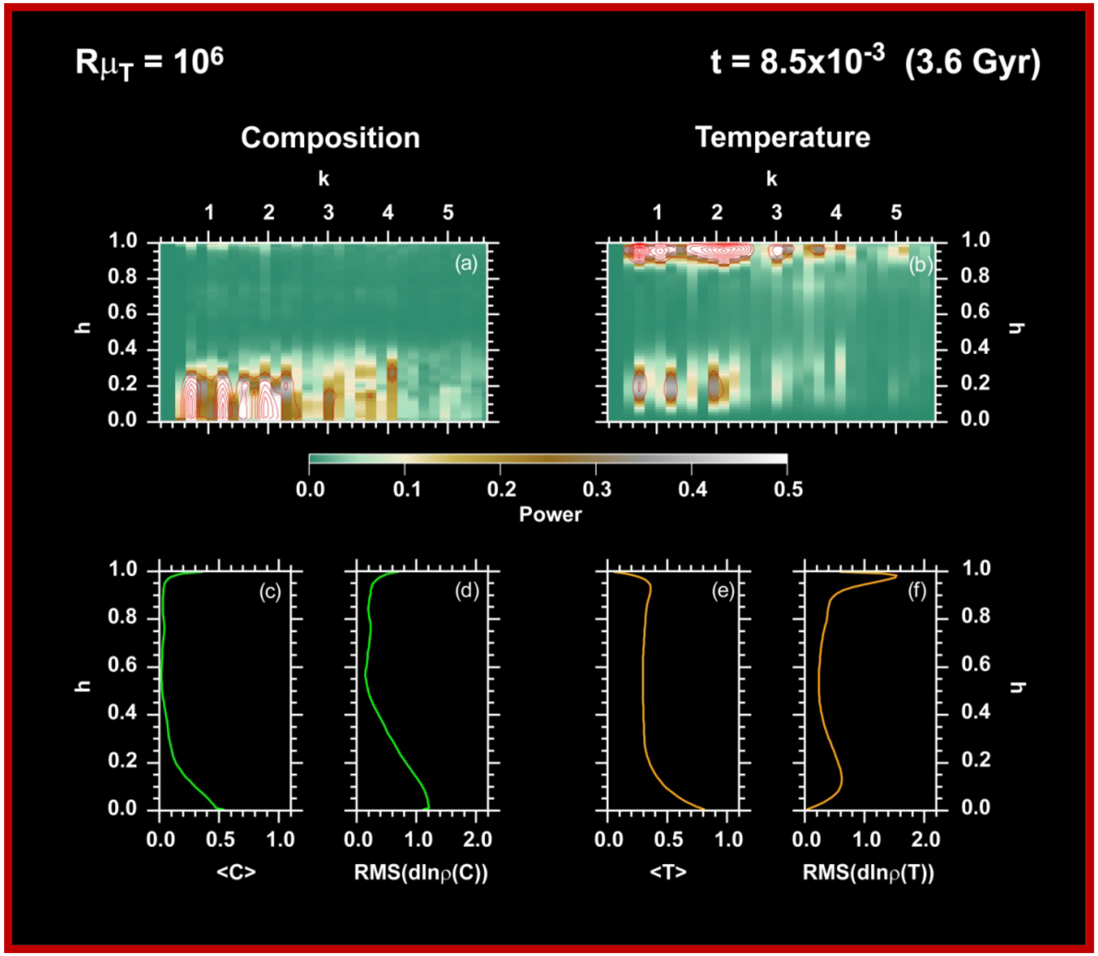

Endothermic phase transition at 660-km depth

Negative Clapeyron slope (-1.0 MPa/K and less):

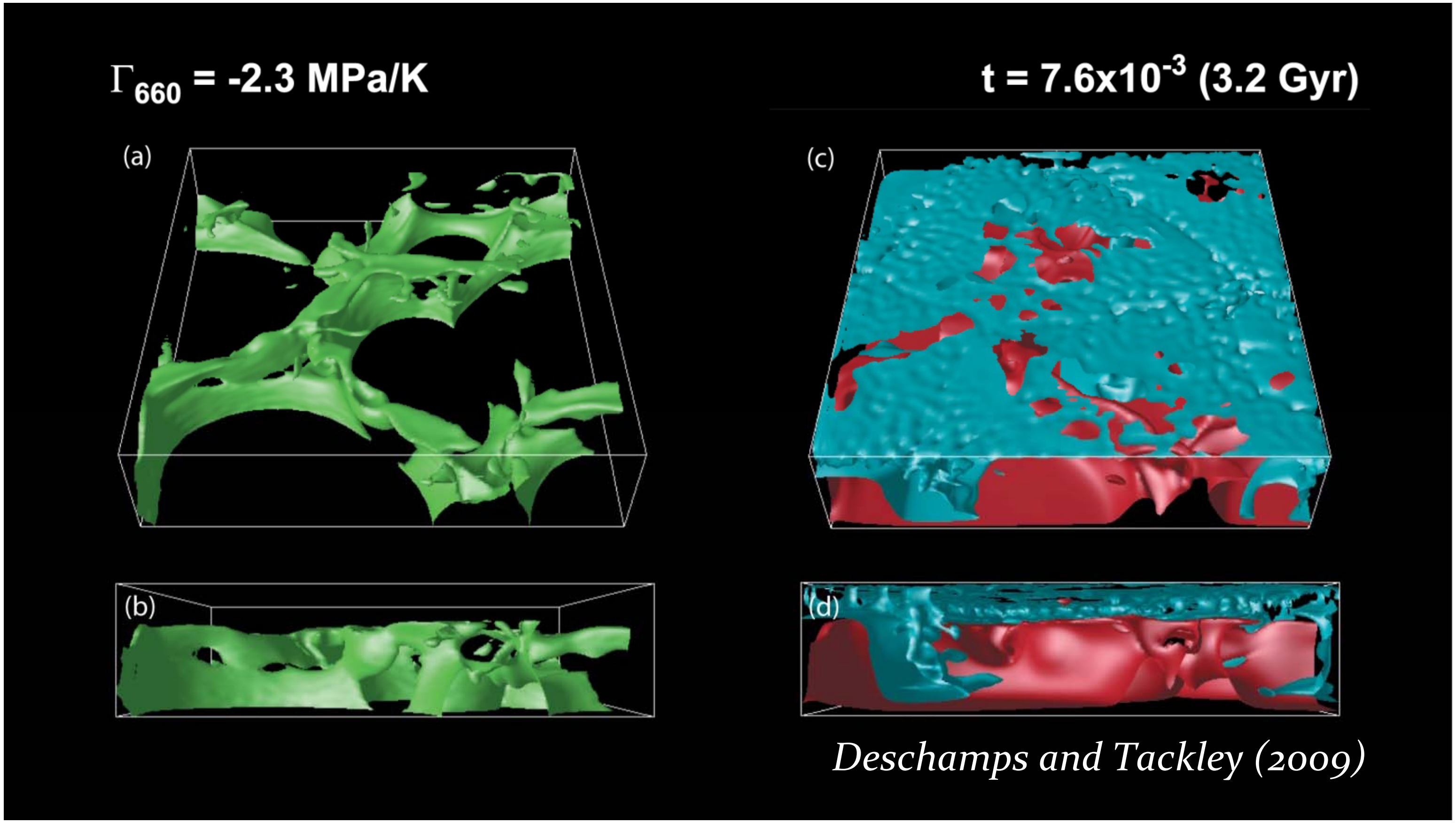

Dense material is trapped below the phase transition. Large compositional anomalies are maintained for a long period of time.

Endothermic phase transition at 660 km depth
(*Profiles & spectral heterogeneity maps*)

- The chemical structure is dominated by strong compositional anomalies at the bottom ($h < 0.2$) of the system ....

… and moderate anomalies below the phase transition.

- The Thermal structure is dominated by moderate thermal anomalies below the surface and at the bottom of the system.

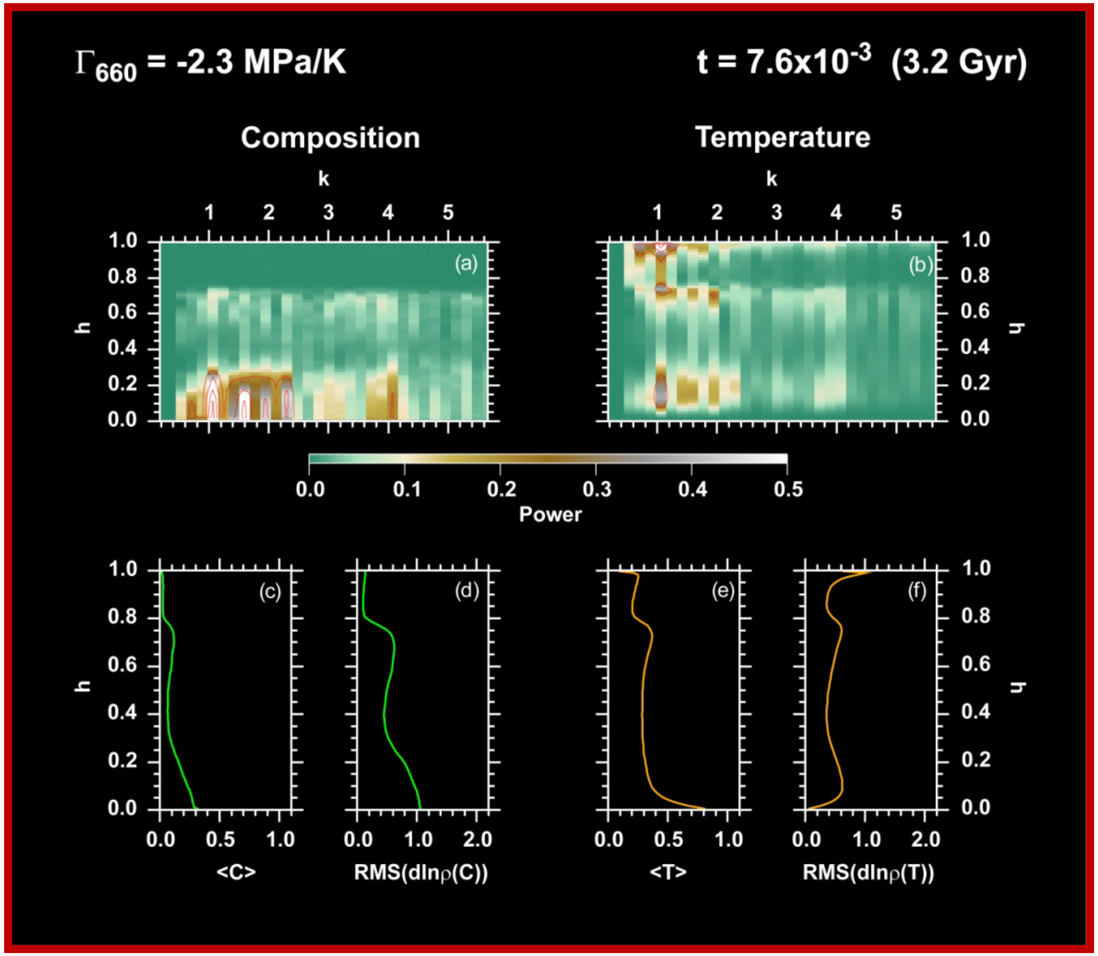

Primitive reservoirs: thermo-chemical distributions

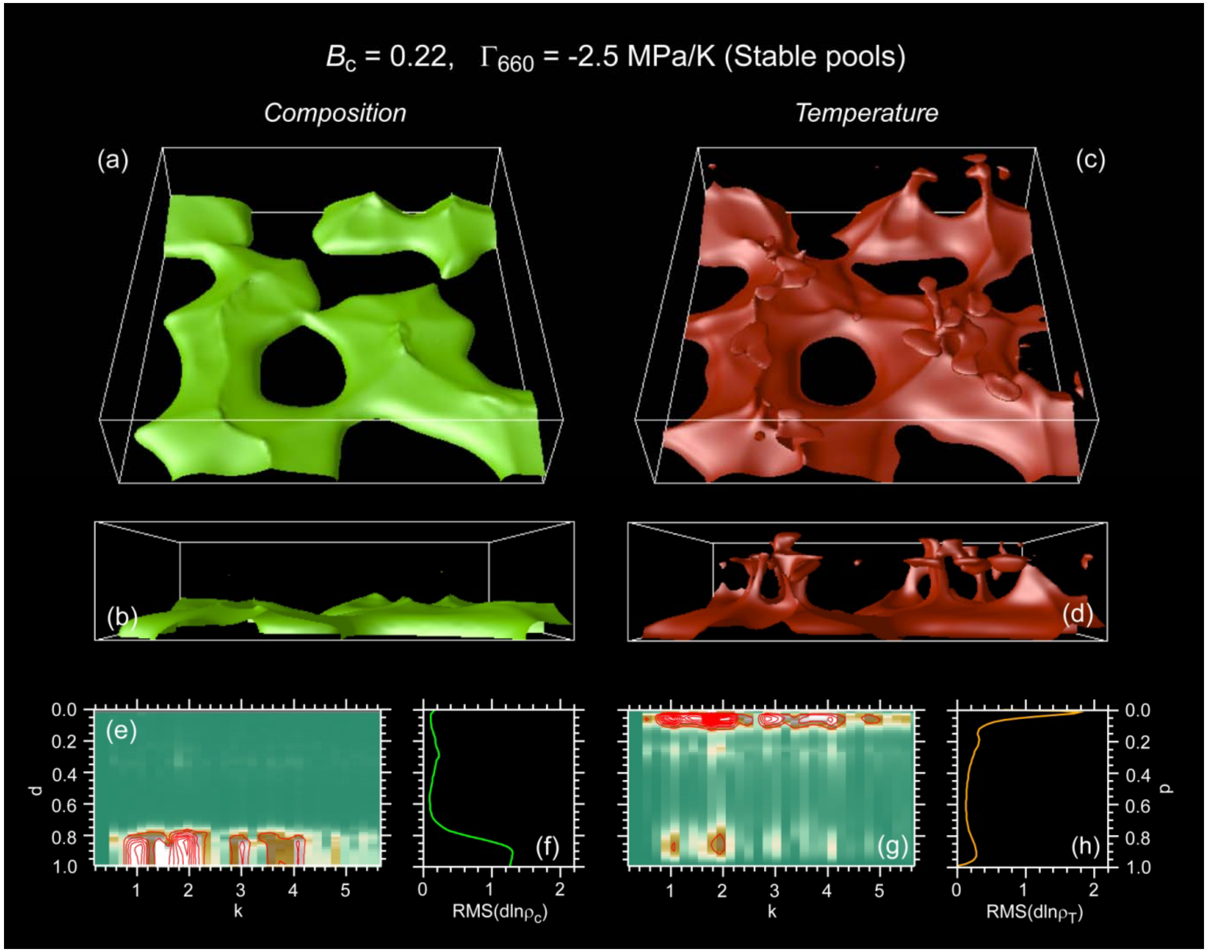

- Large pools of primitive material are generated in the lower mantle and survive convection.
- Most of the dense material remains below the phase transition.

Strong thermal and chemical density anomalies at the bottom of the system

Primitive reservoirs: seismic signatures

- Primitive material enriched in iron (up to 3%), and perovskite (up to 20%):

- dlnV_S and dlnρ up to 2% and 1%, respectively.

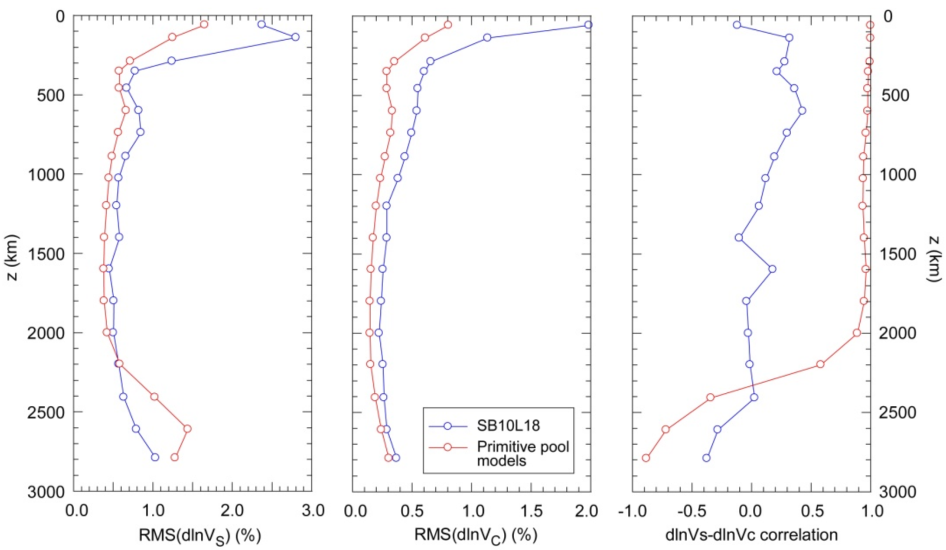

- RMS profiles of dlnV_S and dlnV_C consistent with SB10L18 *(Masters et al., 2000)*.

- dlnV_S and dlnV_C anti-correlated in the lowermost mantle.

- Correlations between vertically averaged velocity and density anomalies in lowermost (2000 ≤ z ≤ 2891 km) layer :

γ = 0.56 and γ = 0.49

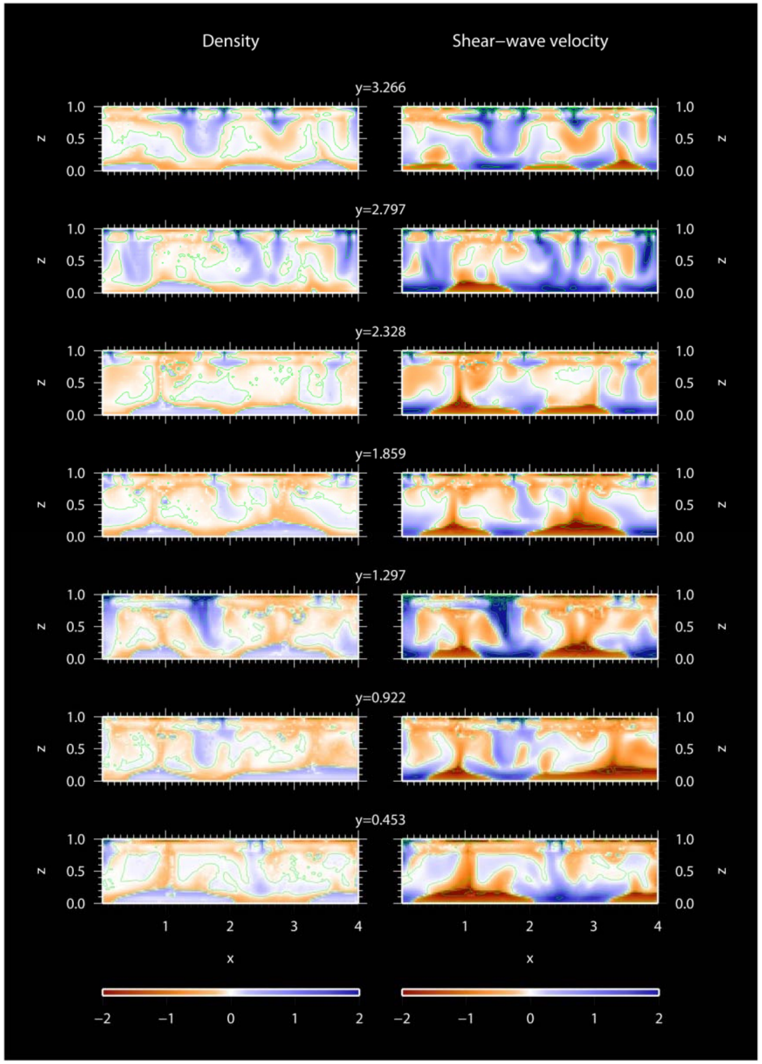

Power spectra

- Models that includes large thermal viscosity contrast and/or a negative Clapeyron slope at 660 km explain well probabilistic tomography ...

- ... except for the chemical density anomalies in the layer 660-1200 km.

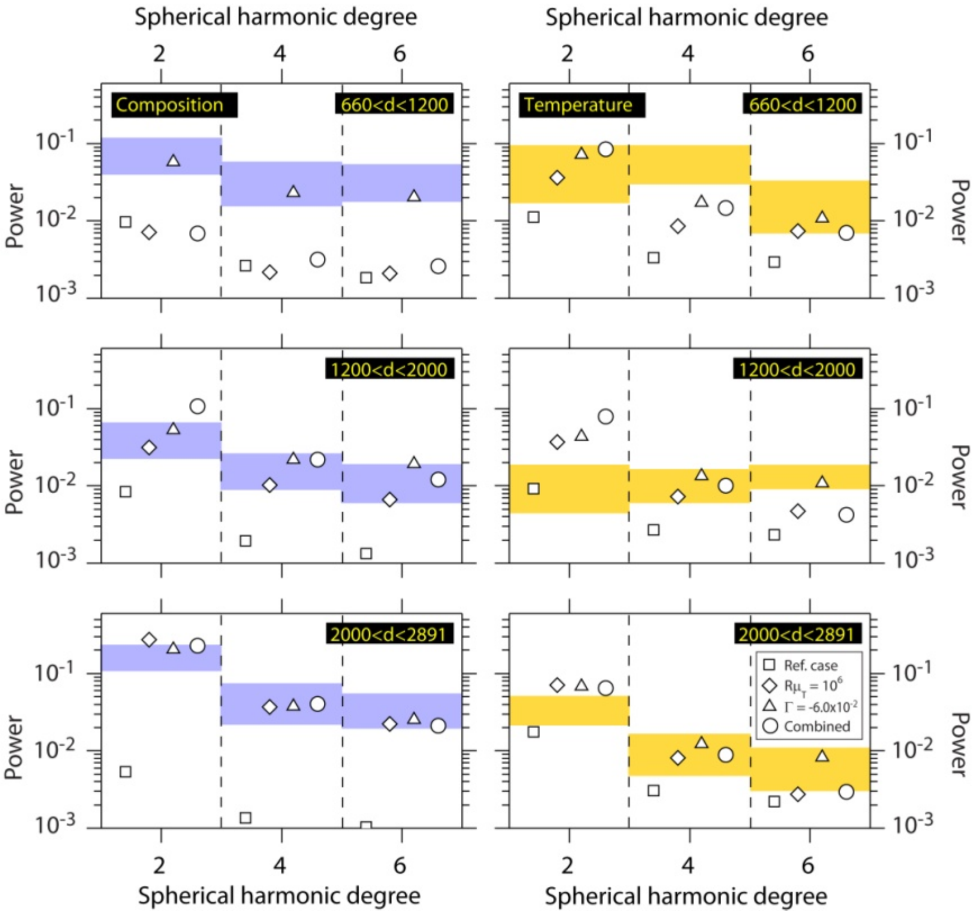

Time averaged power spectra over 1.0 Ga (Deschamps and Tackley, 2009)

Chemical signal of slabs stacked around 700-1000 km ?

Slab recycling

- How to maintain reservoirs of recycled MORB in the deep mantle ?

▶ Numerical modeling using STAGYY (Tackley, 2008):

- Solve the non-dimensional conservative equations of mass, momentum, energy, and composition for an anelastic, compressible fluid with an infinite Prandtl number.
- 'Yin-Yang' (3D-Spherical) grid of $64\times192\times64\times2$ points, with 12 tracers per grid-cell.
- Viscosity depends on temperature, depth, and yield stress.
- Crust is generated by melt differentiation and recycled.
- Two type of tracers, one for MORB, one for Harzburgite.
- Core cooling is accounted for.
- Run over 4.5 Gyrs from initial condition (adiabat plus thin TBL).

and with self-consistent calculated mineral physics :

- Phase diagram (including Clapeyron slope at 660 km), density, thermal expansion, heat capacity, and thermo-elastic properties are calculated by minimizing the free energy of the assemblage using PERPLEX (*Connolly*, 2005).

- Thermodynamic database is from *Xu et al.* (2008).

Petrological compositions

- Mantle aggregate is assumed pyrolitic, with 80% Harzburgite and 20% MORB.
- 4 different petrological compositions are tested to account for possible variations in MORB composition.

Table 1: Bulk compositions of MORB and harzburgite in molar %.

	CFMAS-I		NCFMAS-KT: Khan et al. [2009]		NCFMAS-X: Xu et al. [2008]		NCFMAS-G: Ganguly et al. [2009]	
	harz	MORB	harz	MORB	harz	MORB	harz	MORB
CaO	0.9	14.8	0.4	12.74	0.81	13.88	0.07	11.32
FeO	5.4	7.0	5.63	6.66	6.07	7.06	4.81	8.31
MgO	56.6	15.8	56.07	16.39	56.51	14.94	60.49	17.96
Al_2O_3	0.7	10.2	0.28	9.85	0.53	10.19	0.24	9.45
SiO_2	36.4	52.2	37.62	52.47	36.07	51.75	34.39	50.83
Na_2O	N/A	N/A	0.0	1.88	0.0	2.18	0.0	1.88

Reference density profiles at *T* = 1800 K

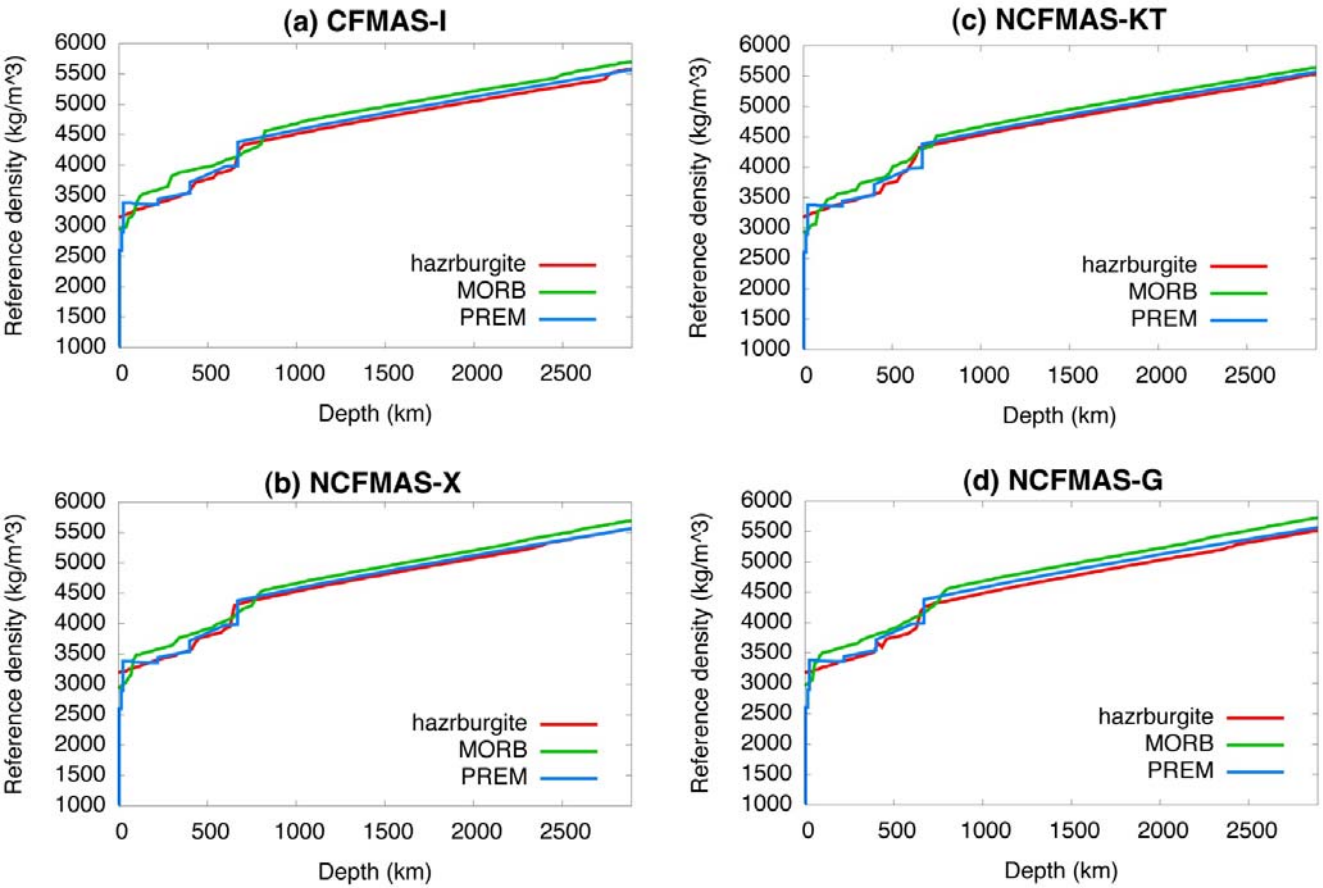

Nakagawa et al. (2010)

- MORB is denser than harzburgite at all depths, except in the layer 660-740 km
  - Small differences, depending on MORB composition

Thermal and compositional distributions

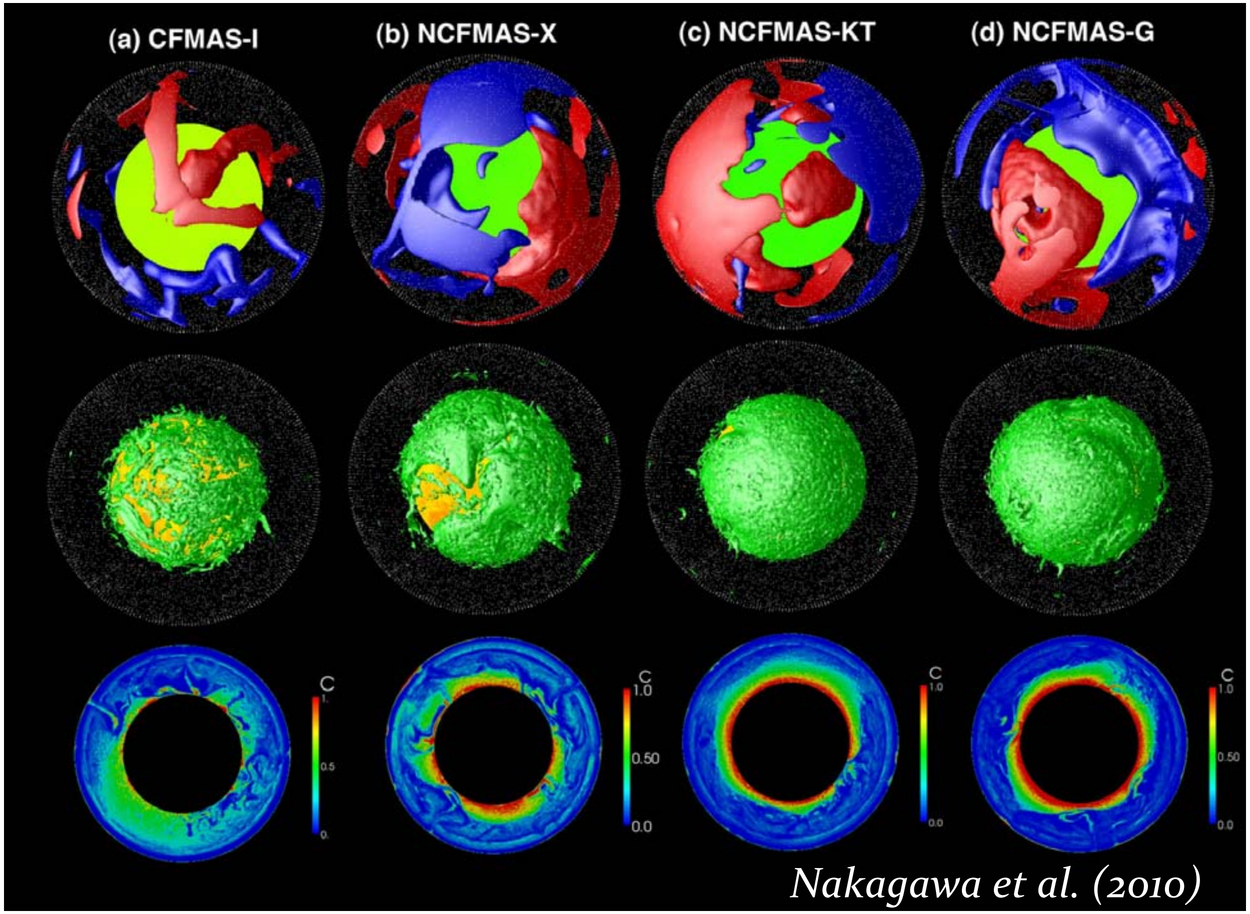

Nakagawa et al. (2010)

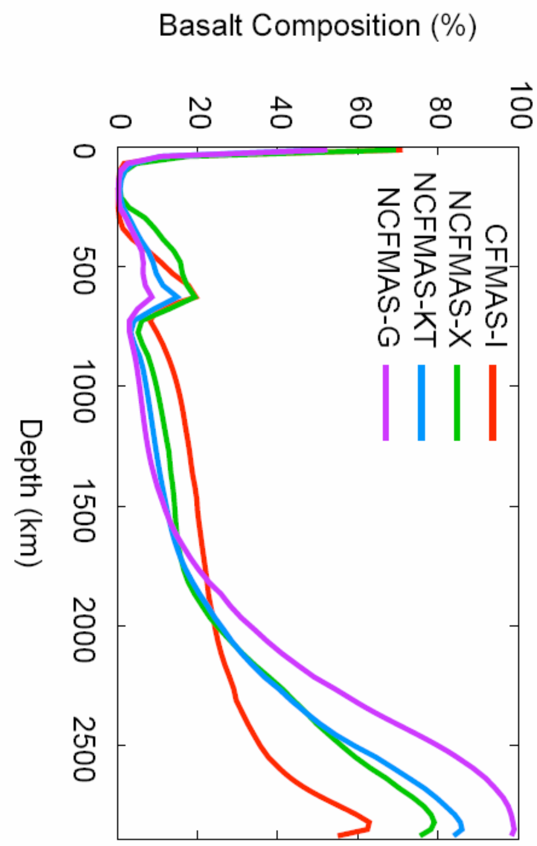

- CFMAS: MORB filtering in the transition zone, discontinuous basal layer of MORB.
- NCFMAS *(Ganguly et al. 2009)*: no MORB filtering in transition zone, MORB segregates in a basal continuous layer.

Synthetic seismic velocity anomalies

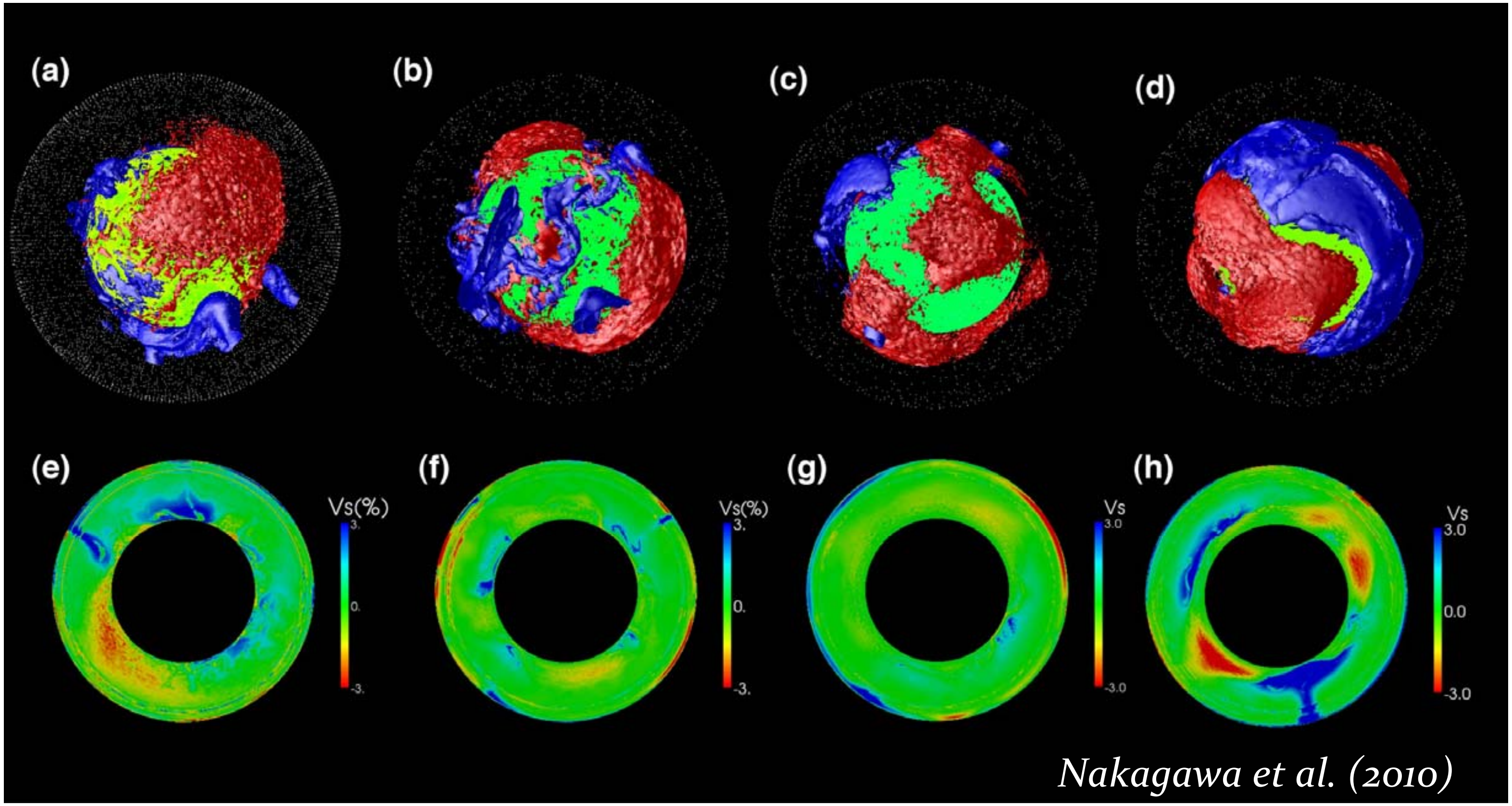

- CFMAS: V_S-anomalies ~3% in amplitude at the bottom of the mantle.
- NCFMAS-X -KT: V_S-anomalies are small throughout the lower mantle.
- NCFMAS-G: V_S-anomalies ~3% in lower mantle, but very small in the lowermost (> 2500 km) mantle.

Some on going works

- Thermo-chemical convection:

- Spherical geometry.

- Model with two sources of chemical heterogeneities (primitive reservoir and recycled MORBs).

- Other observables and constraints:

- Geochemistry and the flux of primitive material entrained in plumes.

- Thermo-chemical distributions and the electric conductivity of the lower mantle.

Primitive reservoirs and spherical geometry

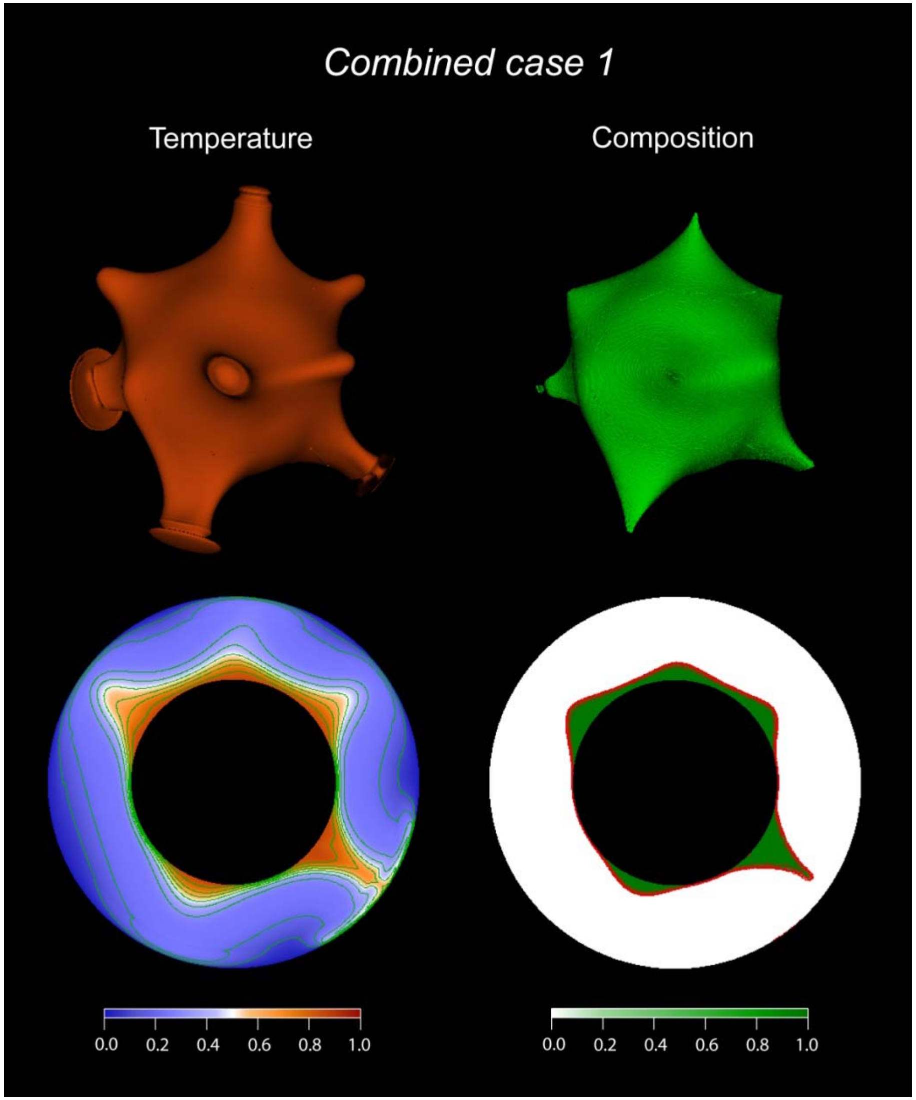

Survival of reservoirs of primitive material is also observed in spherical geometry

Two sources of chemical heterogeneities

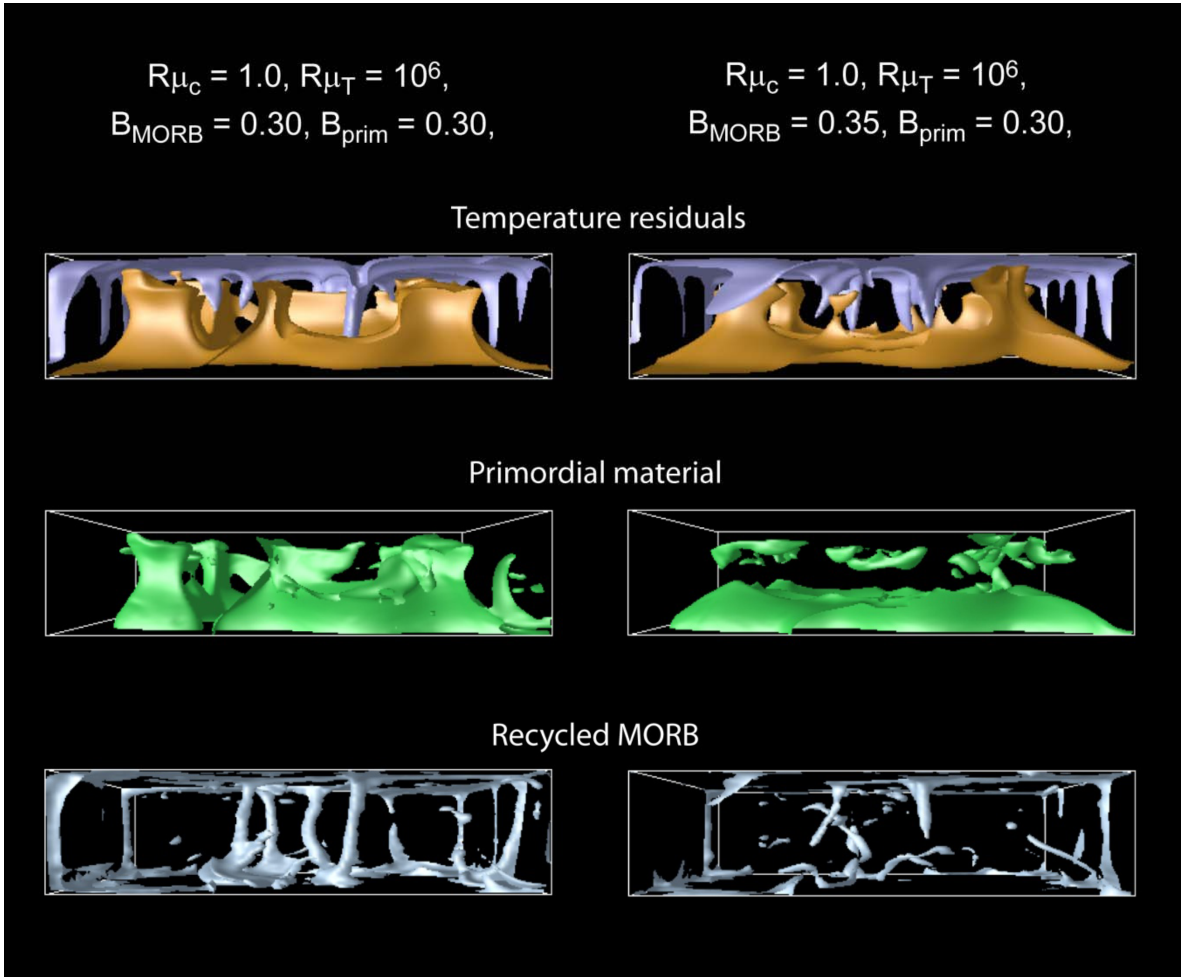

Encouraging, but need to explore more cases ...

Deep mantle reservoirs: hints from geochemistry

- Helium ratio:

- Large dispersion (15000-200000) in $^4He/^3He$ in Ocean Island Basalts (OIB);

- Small ratios sample primitive reservoir *(e.g., Allègre et al., 1995; Hofmann, 1997).*

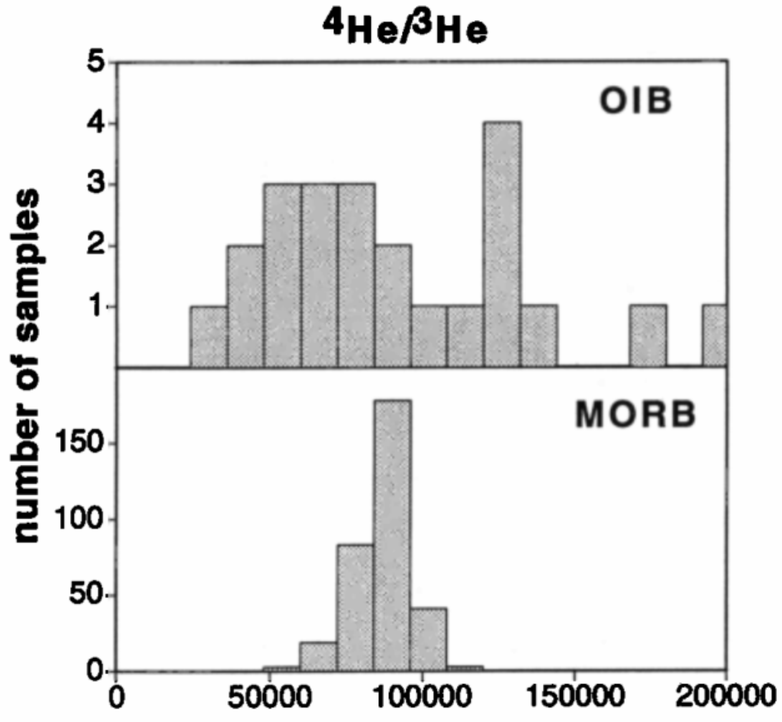

Allègre et al. (1995)

- Incompatible elements:

- OIB are globally richer in incompatible elements, but also show a large dispersion.

- Sr, Nd, and Hf: OIB may partly result from recycled crust.

- Lead data cannot be explained by recycling of continental crust only.

Ocean Island basalts sample several reservoirs, including undegassed reservoir(s) and recycled crust

Entrainment by secondary plumes

- Secondary, thinned, thermal plumes are generated above the phase transition.

- A small fraction of dense material crosses the phase transition upwards and is entrained by secondary plumes.

- The average upwards flux of dense material (relative to total mass flux) is 17% below the phase transition, and 0.3% above.

- Plume entrainment is less than 10%.

Plume entrainment qualitatively supports the hypothesis that OIB partially sample a deep, undegassed reservoir

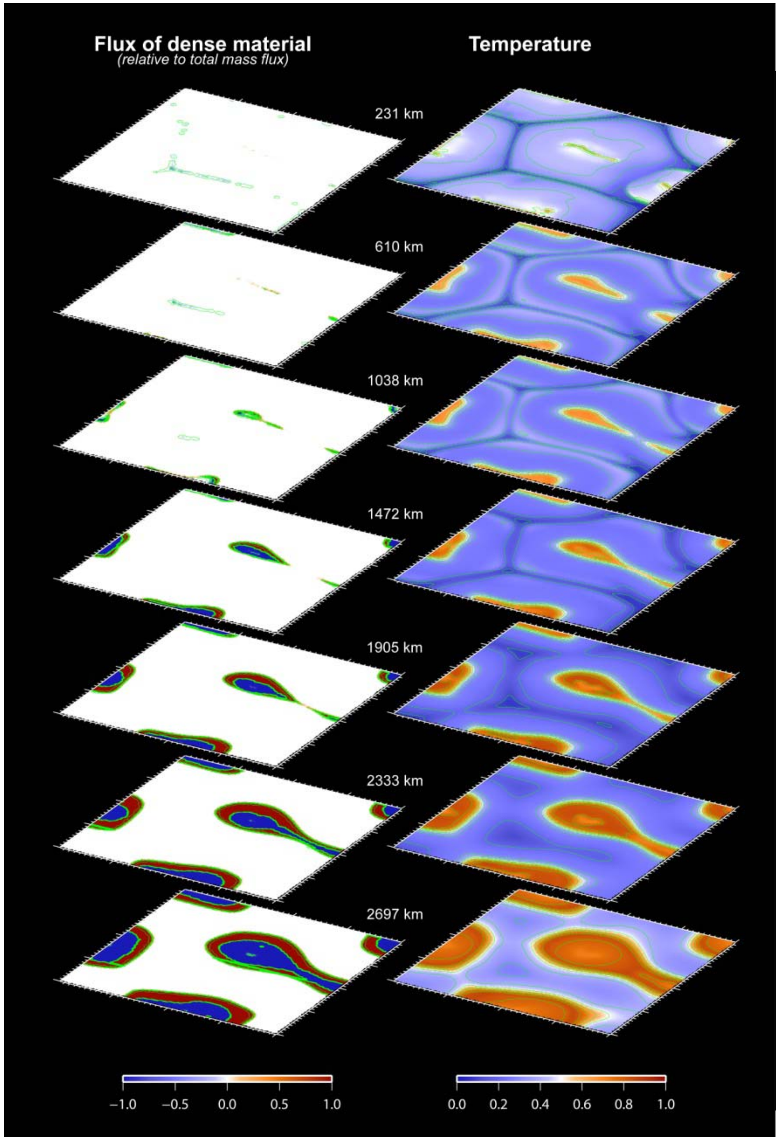

Additional constraints: electric conductivity

- Electric conductivity:

- Increases with temperature
- Depends on composition (iron, perovskite/ferro-periclase)

- Distribution of electrical conductivity in the lower mantle from thermo-chemical anomalies:

- Thermo-chemical distributions (dT, dFe, dX_{pv}) from probabilistic tomography

- Conductivity modeled following Vacher and Verhoeven (2007), and data from Xu et al. (2000) and Dobson and Brodholt (2000).

- Belt of high conductivity around the equator in the deep mantle, but:

- Large uncertainties.

- Amplitude is too small to significantly influence magnetic field variations.

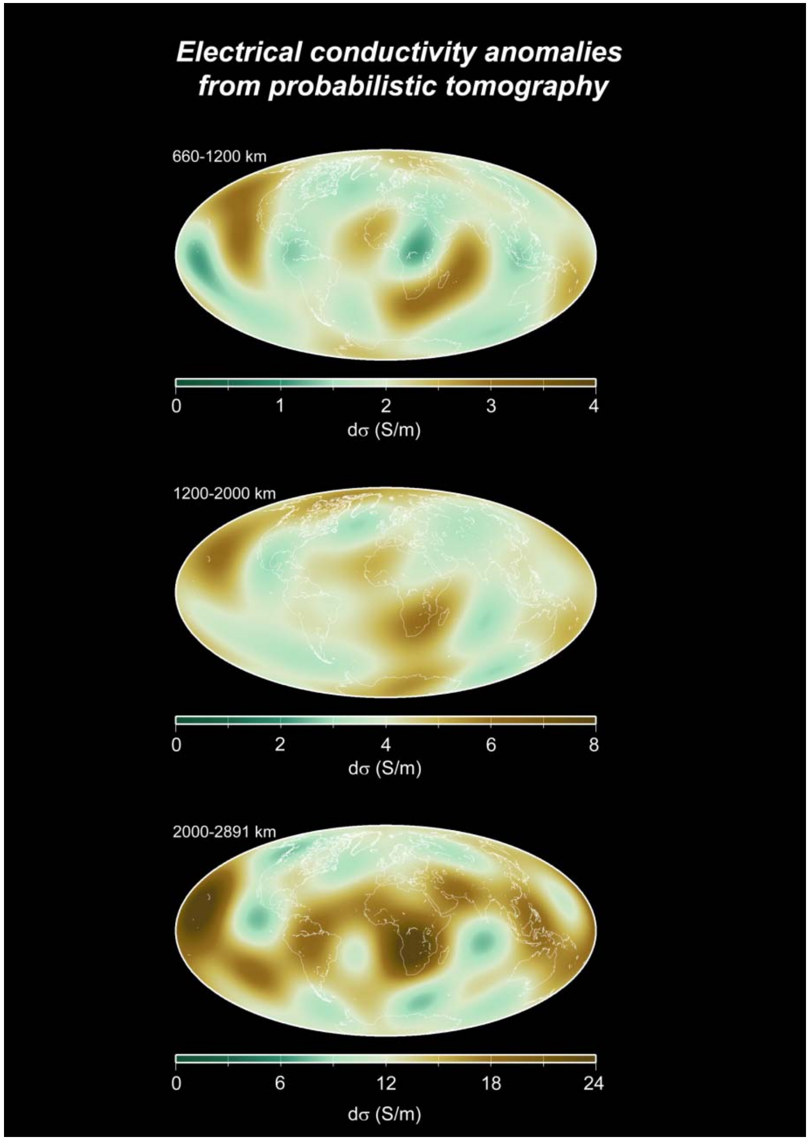

Deep mantle structure and dynamics: conclusions

- The Earth's Mantle is thermo-chemically heterogeneous:

- Lateral variations in composition are needed to explain seismological observations.

- Probabilistic tomography maps thermo-chemical anomalies in the deep mantle.

- Strong lateral anomalies of composition in the lowermost mantle ($z > 2000$ km)

- Reservoirs of dense material can survive convection. Important ingredients are:

- A moderate buoyancy ratio, to avoid stratification.

- A large thermal viscosity contrast, to maintain reservoir of dense material in the deep mantle.

- A negative Clapeyron slope at 660 km, to reduce the upwards flux of dense material. This may also partly the geochemistry of OIB.

- Recycled MORB can accumulate at the bottom of the mantle, but slightly different MORB compositions lead to different structures.

Mantle dynamics

- Thermo-chemical models in spherical geometry …
- … and with several sources of chemical heterogeneities (primitive reservoirs and recycled MORBs).
- Shape and stability of primitive reservoirs.
- Variation of thermal conductivity with temperature.
- Role of post-perovskite.

Mantle thermo-chemical structure

- Detailed nature (iron, MORBs, ppv, …) and origin (slab, early differentiation) of chemical heterogeneities.
- Probabilistic tomography with better resolutions.
- More constraints from mineral physics:
  - Refined thermo-elastic data.
  - Electric conductivity.

Comparison with observables

- Quantify the flux of dense material in plumes, comparison with geochemistry.
- Lateral variations of electric conductivity in the deep mantle, consequences on magnetic field.
- Lateral variations of heat flux at CMB, consequences on core dynamics and geodynamo.

Merci !

Vermeer, 'The Geographer' (1669)